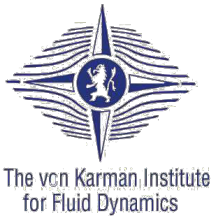

Universitat Politècnica de València
Escuela Técnica Superior de Ingeniería del Diseño

Design of a fast-response temperature probe for turbine measurements

Master's degree Thesis
Aerospace Engineering

Author: Noelia Tarazona Benito
UPV Supervisor: Dr. Pedro Piqueras
VKI Supervisor: Dr. Sergio Lavagnoli
VKI Advisor: Bogdan Cezar Cernat

Brussels, September 2019

Resumen

El aumento del tráfico aéreo conlleva la continua búsqueda de mejoras en la eficiencia de los motores. Dicha eficiencia está directamente relacionada con la temperatura máxima que se puede alcanzar en el proceso de combustión y, por tanto, la temperatura de entrada en la turbina. Las elevadas temperaturas alcanzadas pueden provocar daños en los distintos componentes, de ahí la importancia de la caracterización del flujo en la primera etapa de la turbina de alta presión.

En el instituto de investigación von Karman Institute for Fluid Dynamics cuentan con instalaciones que simulan dicha etapa, el VKI CT3 ring. Esta instalación permite reproducir en términos de números de Mach y Reynolds el flujo existente en una etapa de una turbina de alta presión de un motor de aviación moderno.

El principal objetivo de esta tesis es el diseño de una sonda capaz de medir la temperatura y sus fluctuaciones asociadas al paso de los álabes en las instalaciones antes descritas para poder llevar a cabo la caracterización del flujo y los distintos fenómenos presentes durante esta etapa. Debido al elevado número de álabes y revoluciones, la respuesta de frecuencia requerida es del orden de 25-50kHz.

Tras el estudio de las sondas ya fabricadas y distintos prototipos diseñados se procede con el diseño del prototipo final intentando satisfacer las necesidades establecidas. El diseño completo comprende desde el estudio inicial de dimensionado hasta la configuración de los sensores y análisis del comportamiento térmico de la sonda.

La solución final obtenida es un equilibrio entre todos los parámetros y necesidades. Dicha configuración permite la caracterización de la temperatura del flujo en CT3 con un número limitado de medidas. La futura fabricación de la sonda se realizará en los laboratorios del propio instituto.

Abstract

The increase in air traffic entails the continuous search for improvements in engine efficiency. This efficiency is directly related to the maximum temperature that can be reached in the combustion process and, therefore, the turbine inlet temperature. The high temperatures reached can cause damage to the different components, hence the importance of the flow characterization in the first stage of the high pressure turbine.

The von Karman Institute for Fluid Dynamics has facilities that simulate this stage, the VKI CT3 ring. This installation allows to reproduce in terms of Mach and Reynolds numbers the flow existing in a stage of a high-pressure turbine of a modern aviation engine.

The main objective of this thesis is the design of a probe capable of measuring the temperature and its fluctuations associated with the passage of the blades in the facilities described above to be able to carry out the characterization of the flow and the different phenomena present during this stage. Due to the high number of blades and revolutions, the required frequency response is of the order of 25-50kHz.

After the study of the probes already manufactured and different prototypes designed, the final prototype is designed to meet the established needs. The complete design includes from the initial sizing study to the configuration of the sensors and analysis of the thermal behavior of the probe.

The final solution is a balance between all parameters and needs. This configuration allows the characterization of the flow temperature in CT3 with a limited number of measurements. The future manufacturing of the probe will be carried out in the laboratories of the institute itself.

Contents

Resumen II

Abstract IV

List of figures IV

List of tables VII

Nomenclature IX

I Technical report 1

1 Introduction 3

1.1 Motivation . . . 3

1.2 Precedents . . . 6

1.3 Objectives . . . 7

1.4 Methodology . . . 8

2 Theoretical framework 11

2.1 Temperature measurements . . . 11

2.2 Current instrumentation . . . 11

2.3 Thin films . . . 12

2.3.1 Working principle . . . 13

2.3.2 Previous designs . . . 13

3 Experimental and computational tools 21

3.1 Experimental tools: the CT3 rig . . . 21

3.2 Computational tools . . . 22

4 Results 25

4.1 Design requirements . . . 25

4.2 Thin film sensor options . . . 27

4.2.1 Double layer . . . 27
4.2.2 Single layer . . . 28
4.3 Basic probe parameters . . . 29
4.3.1 Length . . . 29
4.3.2 Diameter . . . 30
4.3.3 Heater hole . . . 32
4.4 Yaw angle sensitivity . . . 35
4.4.1 Flow characteristics around the cylinder . . . 35
4.4.2 Test yaw angles profiles . . . 39
4.5 Cabling . . . 43
4.6 Thin films Joule heating . . . 46
4.7 COMSOL 2D design . . . 47
4.7.1 Static . . . 47
4.7.2 Transient . . . 49
4.8 COMSOL 3D design . . . 52
4.8.1 Probe tip . . . 52
4.8.2 Support . . . 53
4.8.3 Insulation . . . 59
4.9 Final design . . . 61

Conclusions **64**

Future work **66**

II Tender dossier **71**

5 Occupational Health and Safety Ordinances **73**
General rules . . . 73
General conditions of workplaces and protection mechanisms and measures . . . 74

III Costing **81**

1 Introducción **83**

2 Budget balance **85**
Departure from meetings . . . 85
.1 Labour costs . . . 85
.2 Equipment depreciation costs . . . 87

.3 Costs of expendable material 88
Start of validation and analysis 88
.1 Labour costs 89
.2 Equipment depreciation costs 89
.3 Costs of expendable material 90

3 Overall budget **91**

IV Annexes **93**

A Technical drawings **95**

List of Figures

1.1 Brayton Cycle 4
1.2 Work methodology scheme 8

2.1 Oxford double prong probe [5] 14
2.2 Oxford double prong probe scheme [5] 14
2.3 Oxford single prong probe scheme [4] 15
2.4 Zurich entropy probe [14] 16
2.5 Adiabatic wall temperature interpolation [2] 18
2.6 Probe prototype [2] 19

3.1 CT3 facility schematization [2] 21
3.2 CT3 view [18] 22

4.1 Thin films samples made by the VKI technician. 28
4.2 Thermal penetration depth. 32
4.3 2D Probe scheme. 33
4.4 Heat flux scheme for the MACOR substrate [3]. 34
4.5 Flow configuration around a cylinder for Re numbers between 300 and $3 \cdot 10^5$ [10]. 36
4.6 Flow recovery temperature around a cylinder for different Mach numbers [4] 37
4.7 Nusselt distribution around a cylinder for different Re numbers [17] 38
4.8 Error due to flow misalignment for different sensor lengths. . . . 40
4.9 Measurements division and maximum yaw angles for each section. 41
4.10 Scheme of the probe: yaw angle and sensor length [2]. 42
4.11 Slot scheme. 44
4.12 Cabling slot areas computed for different angles. 45
4.13 Final slot scheme. 45
4.14 Temperature distribution with a heat flux imposed of 1060 W/m^2. 48

4.15 Evolution of the temperature distribution after increasing the heat flux produced by the sensor. 49
4.16 Imposed evolution of the values on the sensor surface for the transient studies. 50
4.17 Temperature contours at the end of the test. 51
4.18 Temperature profiles along a line that joins the stagnation point with the back of the probe. 51
4.19 Temperature contours for the 3D MACOR substrate. 53
4.20 New MACOR substrate probe design. 54
4.21 Temperatures map for an attachment of 5mm and Brass support. 55
4.22 Example of plot for sensors gradient temperature calculation. . . 57
4.23 Temperature gradient between thin films vs probe length. 57
4.24 Heater power needed vs probe length. 58
4.25 Temperature distribution for an insulated case. 59
4.26 Temperature gradient between thin films vs probe length. 60
4.27 Heater power needed vs probe length. 60
4.28 Final probe tip design. 61
4.29 Final support design. 62

List of Tables

4.1 Painted thin films characteristics. 28
4.2 MACOR thermal properties [2] 29
4.3 Probe characteristics I 30
4.4 Probe configurations for improving yaw angles sensitivity. 40
4.5 Excel yaw angles study for probe positioning. 42
4.6 Heat fluxes computed for different thin-film joule heating. 46
4.7 Temperatures reached at the stagnation point after imposing a heater heat flux of 1060 W/m^2 and different thin-film joule heating options. 48
4.8 MACOR probe dimensions 61
4.9 Support dimensions 62
4.10 Thin-film sensors characteristics and layout 63

III Costing **83**

2.1 Labor cost associated with project planning meetings 86
2.2 Labor cost associated with doctoral/grantee meetings. 86
2.3 Cost of labour associated with meetings between contracted lecturer, doctor and scholarship holder. 86
2.4 Cost of labor associated with meetings between contracted professor, doctoral candidate and scholarship holder. 87
2.5 Labour cost associated with the departure of meetings. 87
2.6 Cost of equipment associated with the departure of meetings. . . 88
2.7 Equipment and amortisation cost of equipment under the heading of meetings. 88
2.8 Cost of consumables associated with meetings. 88
2.9 Labour cost associated with the validation and analysis item by the doctoral candidate and scholarship holder. 89
2.10 Equipment at the beginning of the validation and analysis process. 89

2.11 Amortization of equipment in the computational study item. . . 90
2.12 Cost of consumables associated with validation and analysis. . . 90

3.1 Total cost of the project applied the VAT associated with the workforce. 91

Nomenclature

Acronyms

$1D$	One dimensional
$2D$	Two dimensional
$3D$	Three dimensional
CFD	Computational Fluid Dynamics
VKI	von Karman Institute

Greek Symbols

α	Thermal diffusivity/Angle between the stagnation point and incidence flow
δ_P	Thermal penetration depth
η	Efficiency
γ	Ratio between heat capacities at constant pressure and volume
ρ	Density

Latin Symbols

A	Area
c	Cord
C_p	Heat capacity at constant pressure
C_v	Heat capacity at constant volume
d	Diameter
E	Energy

Fo	Fourier number
h	Heat transfer coefficient
I	Electrical current
k	Thermal conductivity
L	Length
M	Mach number
n	Number of moles
Nu	Nusselt number
P	Power
p	Pressure
Q	Heat
q	Heat flux
R	Constant of ideal gases
R	Resistance
r	Compression ratio
r	Radius
Re	Reynolds number
s	Entropy
T	Temperature
t	Time
V	Volume/Voltage
W	Work

Subscripts

cond	Conduction
conv	Convection

ext	External
in	Inlet
lim	Limit
o	Initial
out	Outlet
s	Surface
$total$	Total
w	Wall

Part I

Technical report

Chapter 1

Introduction

1.1 Motivation

Air traffic has experienced a very significant increase over the years, today the number of planes flying over our skies is very high. This is associated with serious pollution problems, both acoustic and environmental. Therefore, it is not surprising the great interest that the design of new more efficient aircraft and engines arouses in the aeronautical and aerospace market. This efficiency is linked to the reduction of the noise produced and the pollution emitted by these machines.

This work has as its final objective the collaboration with the pursuit and research of new engines. As indicated above, the main objective of the industry and research centers is to improve its global efficiency and performance. For this, it is essential to understand the basic operation of these machines. As well as the main parameters on which said efficiency and performance depends.

Most aeronautical engines are gas turbines or turbojet engines. These thermal turbomachines base their operation on power cycles such as the Brayton cycle, also known as the Joule or Froude cycle. This is a thermodynamic cycle composed, in its most basic form by an adiabatic compression that would correspond to the compression performed by the fan and the compressor, followed by an isobaric heating stage and an adiabatic expansion, which is the simplification of what happens in the combustion chamber and the turbine respectively. The entire cycle is performed by a compressible fluid [19]. The cycle scheme can be seen in Figure 1.1.

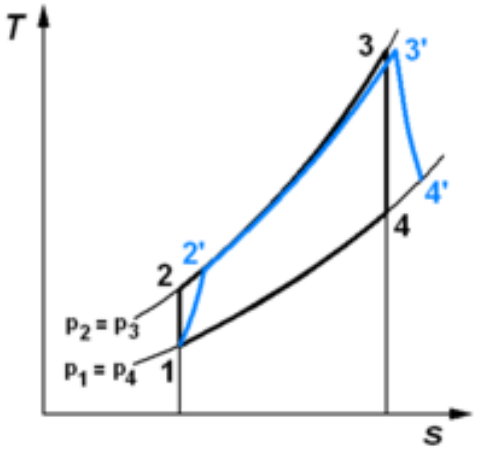

Figure 1.1: Brayton Cycle

The performance or efficiency of a thermal machine is defined as the work obtained (W) from a given applied heat (Q_{in}). To all this, the possible losses or heat transmitted to the environment must be added. For this, the absolute heat is computed by subtracting said heat transmitted to the outside (Q_{out}). With all this into consideration, the definition of efficiency would be the one shown in Equation 1.1.

$$\eta = \frac{|W|}{|Q_{in}|} = \frac{|Q_{in}| - |Q_{out}|}{|Q_{in}|} = 1 - \frac{|Q_{out}|}{|Q_{in}|} \tag{1.1}$$

Taking into account the expressions of incoming and outgoing heat, the performance equation can be obtained as a function of temperature. Knowing that the processes in which such heat transmission occurs happen at constant pressure and that compression and expansion are adiabatic and reversible, Poisson's law is fulfilled. Together with the ideal gas equation ($p \cdot V = n \cdot R \cdot T$) the efficiency can be rewritten so that it depends on the pressures [8]:

$$\eta = 1 - \frac{|Q_{out}|}{|Q_{in}|} = 1 - \frac{nc_p(T_4 - T_1)}{nc_p(T_3 - T_2)} = 1 - \frac{T_1}{T_2} = 1 - \left(\frac{p_1}{p_2}\right)^{\frac{\gamma-1}{\gamma}} \tag{1.2}$$

being γ the ratio between the heat capacities at constant pressure and volume. The final equation that would govern the efficiency of the cycle would be the one shown in Equation 1.3, where r is the compression ratio.

$$\eta = 1 - \frac{1}{r^{\frac{\gamma-1}{\gamma}}} \tag{1.3}$$

Once efficiency is known, the work that can be extracted from said thermal machine can be defined as:

$$\frac{L}{c_p \cdot T_1} = \frac{T_3}{T_1}\left(1 - \frac{1}{r^{\frac{\gamma-1}{\gamma}}}\right) - \left(1 - r^{\frac{\gamma-1}{\gamma}}\right) \tag{1.4}$$

Taking into account that T_1 is the compressor inlet temperature. Therefore, it will depend on the ambient temperature, and thus, the flight height. This means that the main variable on which the final work obtained by the engine depends is the temperature at the exit of the combustion chamber. The higher the temperature said is, the greater the amount of work extracted by the machine.

Currently, temperatures of up to 1800 K can be reached, even more in the military industry. As increasing this temperature implies extracting more work, the trend throughout history has been and will continue to increase. The main problem with this tendency is that there are certain limitations: the limit temperature that is able to withstand the early stages of the high-pressure turbine. These limitations are both thermal and mechanical since normally the temperature increase also implies pressure increases. In addition to the high temperatures and pressures, it should be taken into account that we are facing a rotary machine. This implies that there will be periodic fluctuations due to the periodic passage of the blades.

To improve the design and behavior of these stages, it is necessary to study in-depth the phenomena that occur inside in order to achieve the characterization of the flow in them. Research is currently underway to understand the phenomena and characteristics of the flow at these stages. The purpose of these studies is to improve the thermal resistance of the materials used and the mechanical properties of the components that formalize the stages, especially the first stages of high-pressure turbines. The main objective is to continue increasing the combustion chamber outlet temperature without sacrificing good performance and machine life.

As mentioned before, it should be taken into account that we are facing a

rotating machine, this implies that the flow is not constant. There are fluctuations due to the passing of the blades and these should be able to be measured and characterized. Hence the need to develop new probes and techniques to measure temperature and pressure with a high temporal resolution, being capable of measuring fluctuations of even 10 and 25 kHz.

Throughout this thesis, an attempt will be made to develop a probe prototype for non-stationary temperature measurements in the CT3 facility of the von Karman Institute for Fluid Dynamics, an installation that will be explained later in section 3.1. This probe will be used for a future experimental study whose main objective is to characterize the flow and phenomena that may appear in the early stages of high-pressure turbines.

1.2 Precedents

This project is part of a series of projects carried out by the von Karman Institute for Fluid Dynamics. The works carried out by Bassignana M., Carvalho A.J., and Sciamanna C.[2, 6, 18] are among them, being the most recent ones.

The mainstay of this project is based on the first designs developed by D.R. Buttsworth and T.V. Jones as the start of high-frequency response probes. After this, it is worth highlighting the different designs found in the literature: Oxford double thin-film [5], Zurich high response entropy probe [12] and Stuttgart high response temperature probe [1].The three designs share theoretical foundations but the final designs obtained for each case are different, as it will be seen in section 2.3.

Due to its great importance for the compression of the one-dimensional model, which simulates the probe as a semi-infinite solid, used to obtain the final heat transfer and temperature, it stands out [14] and [9]. In this project, no calculations were made but the model had to be understood beforehand in order to consolidate the knowledge about the working principles of thin-film sensors.

As for the distribution of pressures, Nusselt numbers, recovery temperature and flow characteristics in general around a cylinder to be able to subsequently

understand the best configuration of the different sensors against the flow, it is important to mention the studies summarized in [4]. It is worth bringing up [13] and [14] since the probe exposed in these articles is the first one found in the literature with an azimuthal position of the sensor, therefore it is the first place where we find references to the importance of place the sensor in a position where Nusselt numbers distributions are regular and constant. Therefore, name [17] and [11] because of its importance in obtaining the distribution of Nusselt numbers around a cylinder for different Reynolds numbers.

Finally, highlight the importance of the first designs and studies carried out in COMSOL Multiphysics by M.Bassignana in [2] for their contribution to the understanding of the program and the link modules with Matlab. As well as the technical drawings and first designs made by J.A. Carvalho in [6], for his involvement when comparing designs already made in the institute by the same technicians.

1.3 Objectives

The objectives set at the beginning of the work were focused on the complete design of a temperature probe for subsequent manufacturing and calibration at the von Karman Institute for Fluid Dynamics CT3 facility. Subsequently, as progress was made on the subject, the project was reduced to only the final design of the temperature probe, eliminating the experimental part.

The probe to be designed is designed for a future experimental campaign that requires a certain minimum spatial resolution. Taking into account the future use of the probe, the final objectives are outlined as follows:

- Bibliography study: collect all possible information about previously manufactured probes.
- Decide the final shape of the probe and its dimensions, as well as substrate material.
- Define the type and material of the sensor.
- Design the probe sensor layout and arrangement. Study the number of possible sensors that can be included in the probe to achieve a sweep of the total span length with the least possible number of measures and without sacrificing spatial resolution.

- Study the dimensions and final position of the sensors taking into account the flow characteristics in which the probe will be during the tests.
- To preheat the probe to a certain temperature and to be able to perform the measurements it is necessary to introduce a heater into the probe: determine the power and characteristics of said heater for the different possible temperatures and configurations.
- Analysis of the probe thermal performance.
- Mechanical design and preparation of technical drawings of the probe prototype for manufacturing.

1.4 Methodology

In order to achieve the objectives set in an efficient and orderly manner, the following scheme shows the proposed methodology to carry out the project:

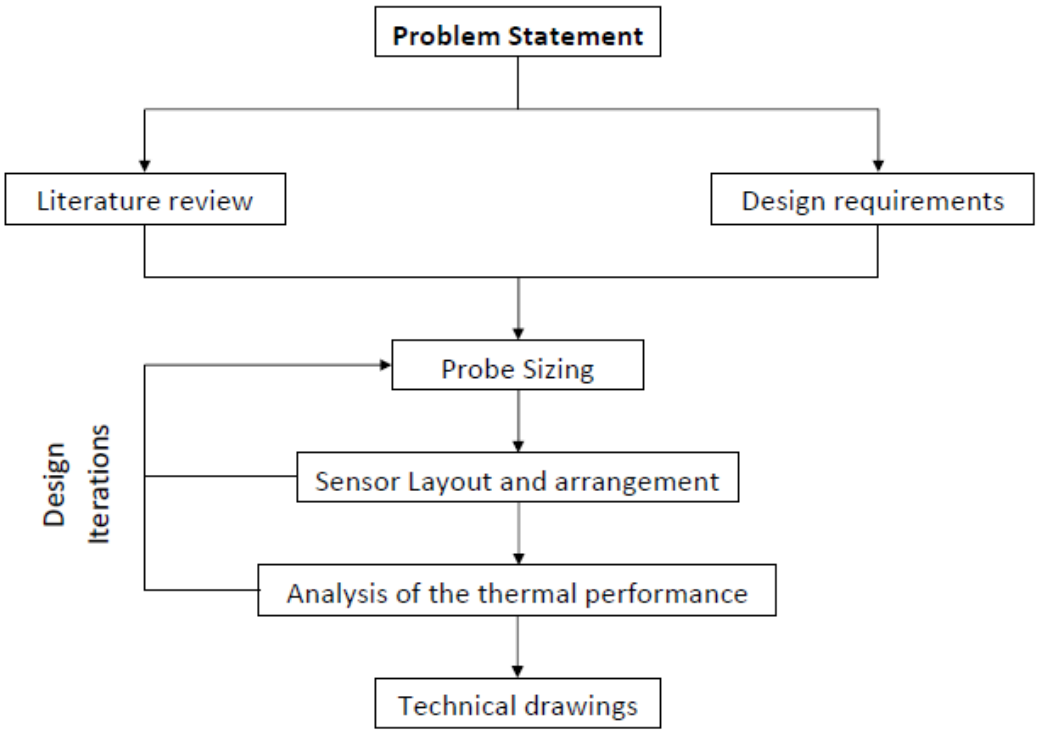

Figure 1.2: Work methodology scheme

The Figure 1.2 shows the initial scheme of the work organization where, initially and after the problem is presented, a bibliographic study is carried

out on temperature probes and, more in-depth, on the thin-film probes already existing. In parallel, the requirements for the probe design are also established.

After these previous steps, the probe is pre-dimensioned, where the length, diameter, and position of the heater will be determined, mainly.

Once the preliminary dimensioning is set, the design and arrangement of the sensor are studied. This is done based on the characteristics of the flow found during the experimental test. If the number of sensors or properties of these changes, it is required to recalculate the previously established dimensions as an iterative process.

The next step will be the thermal analysis of the probe, the behavior that it may have in static and transient conditions, as well as the effect of adding the support to the final temperature distribution. The study of adding some type of thermal insulation between both probe components: MACOR prong tip and support is also included in this part. At this point, again, if one of the probe dimensions changes the design must be iterated.

Finally, once all the characteristics of the probe have been determined, the technical drawings will be made in Inventor for further discussion with the technician.

Chapter 2

Theoretical framework

2.1 Temperature measurements

Nowadays, different techniques have been developed to measure the total flow temperature. The simplest method is based on the thermoelectric effect or Seebeck effect.

This effect is the direct conversion of the temperature difference to an electric voltage and vice versa. A thermoelectric device creates a voltage when there is a temperature difference on each side. On the contrary, when a voltage is applied, it creates a temperature difference. The direction of heating or cooling is determined by the sign of the applied voltage. [20]

2.2 Current instrumentation

There are currently several existing probes that base their temperature measurement on the Seebeck effect. Among them are thermocouples, cold wire probes, and thin-film probes.

Thermocouples

A thermocouple is an electrical device consisting of two dissimilar electrical conductors forming electrical junctions at differing temperatures. A thermocouple produces a temperature-dependent voltage as a result of the thermoelectric effect, and this voltage can be interpreted to measure temperature.

It is known as a thermocouple a transducer formed by the union of two different conductor metals that produce a potential difference from which the temperature difference between both ends can be obtained. This is due to the thermoelectric effect that produces a temperature-dependent voltage [23]. They are very economical, simple instruments and allow measuring a wide range of temperatures, but are very limited by their accuracy and temporal resolution.

Cold wire probes

The cold wire probes also base their operation on the principle that the resistance of a certain material varies with its temperature. In this case, as the name itself indicates, the material used is a conductive wire. They have a higher frequency response but the main disadvantage of this method is that the cable is very sensitive and would not withstand the complex conditions in which the tests are carried out.

Thin film probes

Finally, there are thin film probes. This method is more robust, easy to operate and allows a much higher temporal resolution, reaching frequency response orders of up to 50kHz. The main drawback is that a specific design is needed depending on the application (as you will see in the subsection 2.3.2). The operation principle is similar to that of the previous instruments, its operation for the heat transfer and temperature calculation is based on Newton's convection laws.

In the following section section 2.3 the operation of this type of probe and the different designs that have already been manufactured will be explained in more detail since, due to its high temporal response capacity, this will be the type of probe that we will design in this project.

2.3 Thin films

As indicated above, due to the characteristics that this type of probe can provide, the final design of this project will consist of thin-film sensors. After

that, we will proceed with the explanation of the principle of operation of these sensors, as well as the main probes that have been designed today.

A thin films sensor consists of a highly conductive material layer, usually platinum or nickel, deposited on an insulating substrate. The thin-film acts as a resistance thermometer and its resistance changes linearly with respect to temperature variations[18].

2.3.1 Working principle

The basic operation of this type of probe is based on the measurement of the wall temperature and heat flow of the probe at different temperatures. By means of a linear interpolation, it is possible to reconstruct the adiabatic wall temperature of the probe which, at the stagnation point, coincides with the total temperature of the flow. That is, with the measurements of heat flows at different wall temperatures it is possible to estimate the total temperature of the flow. The device responsible for measuring heat flow is what we call thin-film: very thin resistance sensors located on the surface of the probe.

There are as many types of thin-film probes as applications since it is necessary to adjust the design to the measurement conditions in which the probe will be working. The main designs found in the literature will be shown below.

2.3.2 Previous designs

Several prototypes and designs have already been manufactured with very varied geometries and configurations, depending on the use that would be given to the sensor. They stand out from them:

Oxford double prong probe [5]

This probe consists on two platinum thin film heat transfer gauges located at the stagnation point of fused quartz substrates, operated at different temperatures. Having two distinct sensors at different temperatures allows to avoid making assumptions about the magnitude of the convective heat transfer coefficient and the need of a heat transfer law calibration. Figure 2.1 shows

how the final probe design looks like.

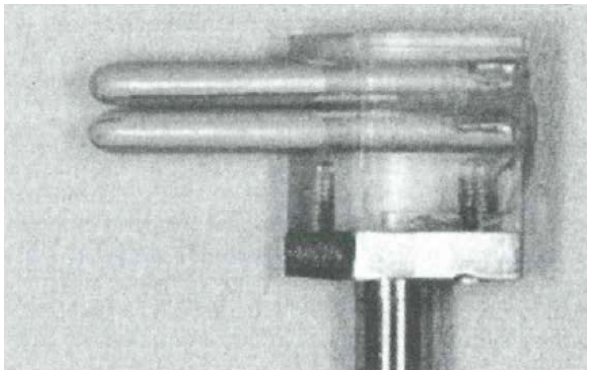

Figure 2.1: Oxford double prong probe [5]

The different temperatures on each thin film are achieved thanks to a heater located on the top prong. Figure 2.2 shows the scheme where the heater can be seen. This heater allows temperature differences up to 50K between both gauges. By having two sensors at different temperatures, two wall temperature histories and heat fluxes can be acquired during one only test.

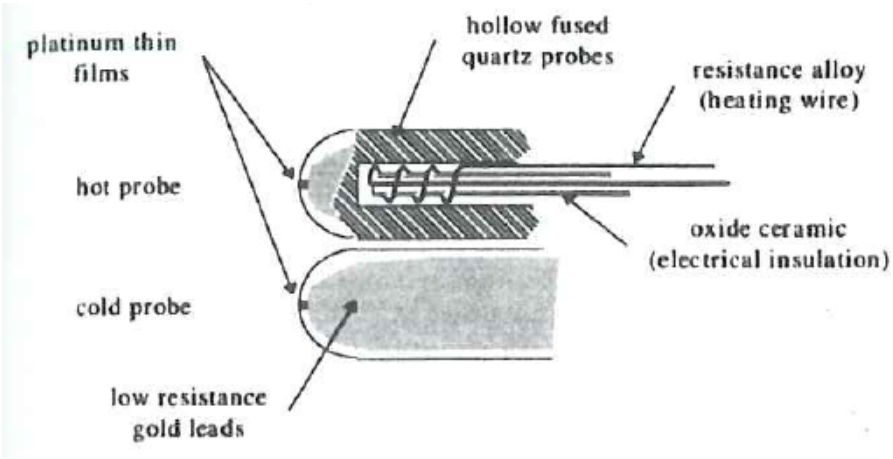

Figure 2.2: Oxford double prong probe scheme [5]

The convective heat transfer is proportional to the temperature difference between the flow total temperature and the probe surface temperature:

$$q = h \cdot (T_{total} - T_{wall}) \tag{2.1}$$

The first step is to know the surface temperatures, which are measured thanks to the voltage across each thin film (Seebeck effect). After that, the convective heat fluxes are computed from the thin film temperature histories

using numerical methods. Since both thin films are under the same flow conditions, same convection coefficient h can be assumed for both cases:

$$q_1 = h \cdot (T_{total} - T_{wall_1}) \tag{2.2}$$

$$q_2 = h \cdot (T_{total} - T_{wall_2}) \tag{2.3}$$

Solving the equation system composed by Equation 2.2 and Equation 2.3 the final value for the convective heat transfer coefficient and flow total temperature can be obtained:

$$h = \frac{q_1 - q_2}{T_{wall_2} - T_{wall_1}} \tag{2.4}$$

$$T_{total} = T_{wall_1} + q_1 \cdot \frac{T_{wall_2} - T_{wall_1}}{q_1 - q_2} \tag{2.5}$$

Where the convective heat flux is estimated with the electric current and the potential difference of each thin film:

$$q_{conv} = q_{total} - I\Delta V \tag{2.6}$$

After some test the accuracy of the probe can be fixed at ± 1 K, with response frequencies detected of 182 kHz.

Oxford single prong probe [4]

The main difference between the previous probe is that this one has two thin film gauges located close to the stagnation point but in only one prong. Figure 2.3 shows the scheme of this prong.

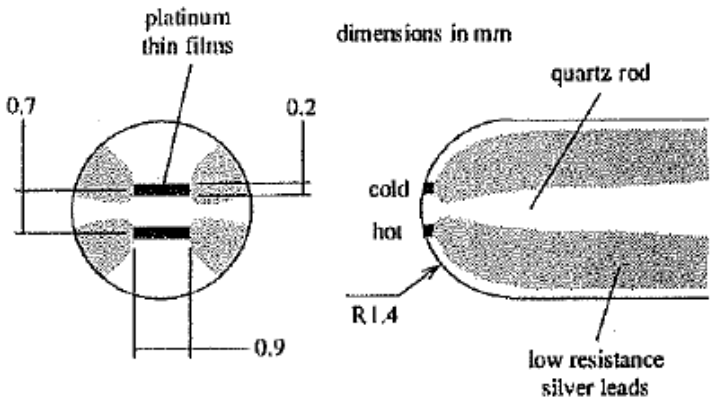

Figure 2.3: Oxford single prong probe scheme [4]

This design allows a better spatial resolution. The two thin films separation distance is less than 1 mm.

The principles of operation and equations that rule the behaviour of this probe are the same than the double one. For obtaining the flow total temperature the two thin films have to operate at different temperatures. In this case the difference is achieved heating one of the gauges with a current pulse of approximately 70 mA. Additionally, each thin film has a different resistance and they are fed by distinct currents to ensure diverse temperatures during all the test. The temperature gradient created between the thin films can reach 120K.

Zurich entropy probe [14, 13]

This probe is a miniature unsteady entropy probe, designed for evaluating the entropy fluctuations in a test facility that simulates a centrifugal compressor stage. The probe has two different components that can be seen in Figure 2.4: a one-sensor fast-response aerodynamic probe and a pair of thin-film gauges.

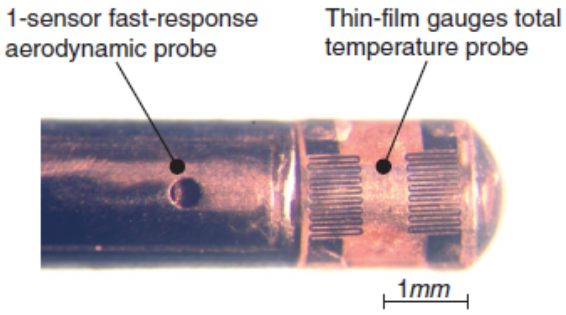

Figure 2.4: Zurich entropy probe [14]

The test conditions force the probe to be able to work a long time in equilibrium with the flow. For obtaining the entropy measurements both a high response temperature and pressure sensors are coupled, because entropy can not be measured directly. The next equation shows how entropy can be computed from temperature and pressure values:

$$\Delta s = c_p \cdot ln\frac{T}{T_{ref}} - R \cdot ln\frac{p}{p_{ref}} \tag{2.7}$$

The working principle is the same as the Oxford one. The only difference is that, as said before, during the test the probe is in thermal equilibrium with the flow. In this case, the diverse wall temperatures are reached by providing distinct electrical currents to each thin film.

Stuttgart probe [1]

This probe is also a high response temperature probe, its principle is basically the same than the previous ones but with one essential difference: in this case there is only one thin film mounted in the probe.

Having only one thin film provides higher spatial resolution and avoids all the possible problems related with interference between thin films that we could find in the previous designs.

Some disadvantages should be considered too. For this probe is necessary to run at least two tests at the same flow conditions to obtain the adiabatic wall temperature. The process is the same but in this case, for having the two different temperatures the test has to be run twice changing the constant current that feeds the thin films.

Once the wall temperatures (T_{wall_1}, T_{wall_2}) of the sensor at the different currents are computed from the voltage drop and current at each point, the equations for the convective heat can be written:

$$q_{conv_1} = h_1 \cdot (T_{total} - T_{wall_1}) \tag{2.8}$$

$$q_{conv_2} = h_2 \cdot (T_{total} - T_{wall_2}) \tag{2.9}$$

considering that the local heat transfer coefficient does not change between the two different measurements, the procedure for the extraction of the total flow temperature is the same contemplated in the previous designs.

VKI Mattia Bassignana [2]

As the design to be carried out in this project is based on the results obtained by Mattia Bassignana, the main characteristics of the probe developed along [2] will be summarized below.

Due to the high demands regarding temporal resolution, the chosen technology is also thin films. In this case, the use of single thin films is considered, as they maximize spatial resolution as well and they avoid problems due to interference between thin films at different temperatures.

As already seen, it is necessary in any case to obtain data for different temperatures. For this design, being a single thin film, at least two tests are required with the same flow conditions but different temperatures in the sensors (as in the probe seen in [1]). The way to establish these temperatures is to introduce a heater inside the probe so that the entire probe substrate can be heated and, with it, the sensors. The system would be similar to the one found in Figure 2.2: a resistive wire wrapped around a cylinder and inserted into the ceramic cylinder that forms the substrate.

This option is chosen as opposed to feeding the thin films with different currents because, by keeping the current constant and equal to that of the design, the noise is reduced and the sensitivity is maximized.

This also allows several tests to be carried out at different temperatures, thus obtaining a much better adjustment and, therefore, greater accuracy. The Figure 2.5 shows how the adiabatic wall temperature would be obtained with better accuracy.

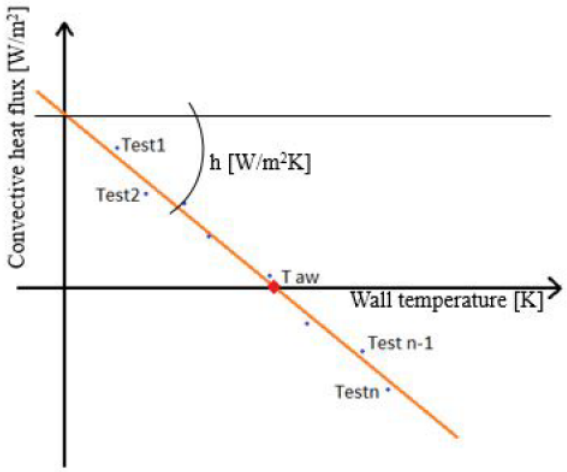

Figure 2.5: Adiabatic wall temperature interpolation [2]

An attempt is made to introduce more than one sensor to limit the number

of measures needed to sweep the entire span, taking into account the possible interference between thin films. The Figure 2.6 shows a photo of the final manufactured prototype. As you can see, in the end only two thin films were introduced.

Figure 2.6: Probe prototype [2]

Chapter 3

Experimental and computational tools

3.1 Experimental tools: the CT3 rig

The CT3 is a blow down tunnel test ring. This facility can reproduce the current flow of a modern aircraft engine high pressure stage turbine in terms of Mach and Reynolds number. It consists of three main elements: the compression tube, the test section and the dump tank. All the elements can be seen in Figure 3.1.

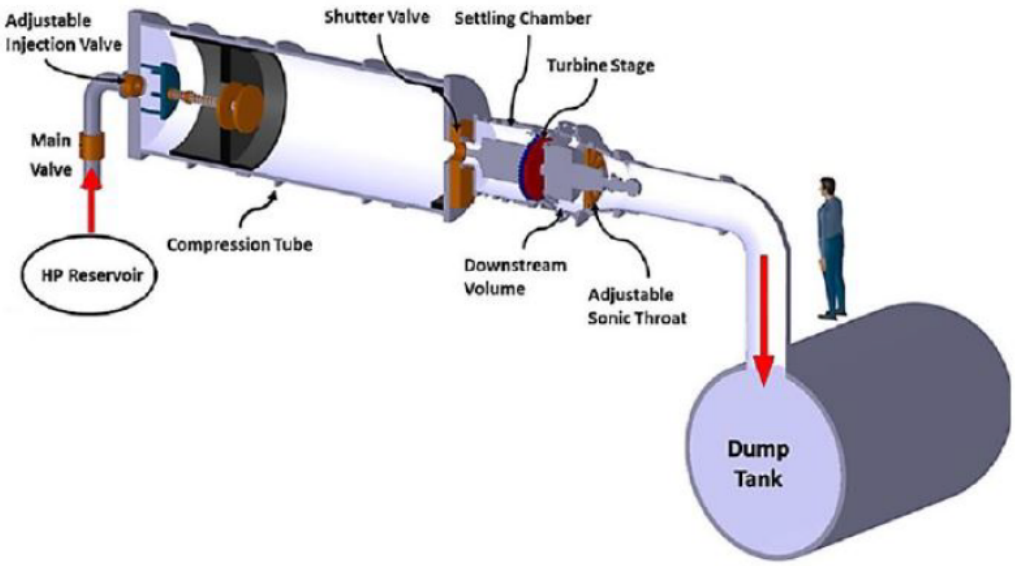

Figure 3.1: CT3 facility schematization [2]

For the separation between the compression tube and the test section an opening shutter valve is used. After the test section an adjustable sonic throat

can be found. This throat is used to control the exiting flow ratio regulating its area, allowing an exiting flow ratio equal to the entering one in the test section. This area is adjusted prior to a test.

Typical test conditions are: first the shutter valve is initially closed, the piston is in the back of the cylinder and the pressure and temperature are regulated to be equal to the ambient one. On the other hand, inside the dump tank almost vacuum conditions are created. Once all the previous steps are fixed, the lubrication system is switched on and the rotor starts to rotate. Pressurized air from the high pressure reserve is regulated and expanded at the back of the cylinder and a quasi isoentropic compression is done by the piston in the compression tube. The moment the ideal pressure is reached the shutter valve opens and the pressurized and hot air is discharged into the test section, recreating the conditions that could be found in a real aircraft engine.

Figure 3.2: CT3 view [18]

3.2 Computational tools

For the computational studies carried out a private software has been used: COMSOL Multiphysics. This software is a general-prupose simulation software for modeling designs, devices and processes in all fields of engineering, manufacturing and scientific research. The platform product can be used on its own of expanded with functionality from any combination of add-on modules for simulating electromagnetics, structural mechanics, acoustics, fluid flow, heat

transfer and chemical engineering. The ad-on modules and LiveLink products connect seammlessly for a modeling workflow that remains the same regradless of what you are modeling [7].

Concerning our main interests, the main (and only) module used of COMSOL Multiphysics was the heat transfer one. Inside this module there are five big domains: heat transfer in solids, heat transfer in fluids, heat transfer with phase change, heat source and initial values. Also different boundary conditions can be applied: temperature, thermal insulation, outflow, symmetry, heat flux, open boundary, inflow heat flux, periodic heat condition, boundary heat source, thermal contact, thin layer, thin film and radiation, diffuse surface. For this project, the only ones used were the heat transfer in solids and initial values domains and heat flux boundary conditions.

For defining the heat flux boundary condition the first step is determine the type of heat flux between the three different available options:

- **General inward heat flux:** the one used for the heater and the thin-film sensors joule heating. The assumed equation for this case is:

$$-n \cdot (-k\nabla T) = q_0 \tag{3.1}$$

  where the heat flux q_0 is the parameter introduced by the user.

- **Convective heat flux:** used for the convection imposed all over the cylinder surface.

$$-n \cdot (-k\nabla T) = h \cdot (T_{ext} - T) \tag{3.2}$$

  where, in this case, the heat transfer coefficient and external temperature were the inputs for the user.

- **Overall heat transfer rate:** this option was not used.

$$-n \cdot (-k\nabla T) = h \cdot (T_{ext} - T) \tag{3.3}$$

$$q_0 = \frac{q_{tot}}{A} \tag{3.4}$$

  q_{tot} is the parameter that should be defined by the user.

Both probe models, 2D and 3D, were implemented in COMSOL in order to know and understand the thermal behaviour of the probe prototype under different conditions. Static simulations were run at the beginning, while at the

end of the thesis some transient ones were carried out trying to replicate the test conditions.

Apart from the studies done in COMSOL, some simple studies were carried out in Matlab, such as the influence of the sensor length on the measurements error, creating arrays that contain the test conditions (temperature and thermal convection coefficient) for the following transient simulations, etc.

Also for the first approaches an excel sheet was developed. Excel was the chosen software due to its easier implementation for parametric studies. The main design constraints were fixed and all the other parameters were computed from the first ones. That way every time a design parameter was changed, all the other ones were recalculated automatically and in a very visual way. This software was used for computing the final number of sensors and their dimensions, total probe length, heater power needed, final temperature approached after turning the heater on, thin-film joule heating and different probe positions to avoid too high yaw angles between the flow and the sensor.

To sum up, three different software were used: COMSOL Multiphysics, Matlab and Excel. The first one for modelling and studying the thermal behaviour of the probe designs, the second one for simple calculations and graphs and the last one for the main parametric studies that based the final probe design.

Chapter 4

Results

In the next chapter, all the work developed throughout the project is compiled, following the chronological order in which it was proposed at the beginning (Figure 1.2). It should be noted that many times at some point it was necessary to change the dimensions or arrangement of some of the parts, such as the final length of the probe. Therefore, the design that will be presented is the end result of many iterations.

The process is basically summarized in an initial study of the design requirements to seek their satisfaction from the beginning. Once the objectives have been established, a bibliographic investigation is first carried out on the designs previously manufactured at the von Karman Institute for Fluid Dynamics, as well as on the different options regarding types of thin-film sensors. A preliminary design is then performed after several parametric studies to determine the main geometric parameters of the probe: length, diameter, dimensions of the hole for the heater, the characteristics of the sensor, etc. Once the geometry is established, the studies are run in COMSOL to characterize the thermal behavior of the probe under different conditions: static and transient. Finally, the technical drawings made in Inventor and the real opinions of the technician before the future manufacture of the probe will be shown.

4.1 Design requirements

As already said during the introduction and the previous chapters, a high temporal and spatial resolution is sought. It is necessary to cover frequencies of up to 25 kHz and ideally be able to cover the clearance tip in terms of spatial terms, that is, 1 mm.

This probe is designed to be used in a future experimental campaign whose main objective is to characterize the flow in the CT3 facility of the VKI. In the section 2.3.2 it has already been determined that the probe to be manufactured will be like those found in [1]: single thin film probe. As already indicated in section 2.3.2 and section 2.3.2, this type of probe implies that two or more measurements have to be made with the same flow characteristics but changing the temperature at which initially thin-films are found. This already implies in itself a greater number of necessary tests, so that another of the design requirements will be to maximize the number of sensors present in the probe, being able to completely sweep the total span length with the least possible number of measurements.

It should be noted that being a probe to be manufactured in the institute itself, it is sought to be easy to manufacture and cheap. In addition, the working conditions of the probe will be very hard, the design must be robust and reliable, capable of withstanding large thermal fluctuations and mechanical stress.

In section 3.1, the facility where the probe will be used, as well as the procedure and general operation to perform a test, have been explained more fully. It must be taken into account that the test lasts a total of 0.7 seconds, with a highly three-dimensional flow, which implies that the probe should not be very sensitive to changes in the angle of attack against the flow. The temperature range in which you should be able to work is between 300 and 380 K and Mach numbers between 0.1 and 0.4.

The ideal error should be 1K or less. It is also important to reduce the intrusiveness of the probe, so the measurements will be as realistic as possible. This implies considering a design with the smallest possible diameter, in addition to a study of how a cylinder of these dimensions would behave in a flow of these characteristics.

Once the main design requirements for the temperature probe have been established, the design itself is carried out in the following sections.

4.2 Thin film sensor options

This project starts from the final design proposed by M. Bassignana in [2]. The main difference between the design to be explained below and his prototype is based on the number of sensors that the probe will contain. In this case more than two sensors will be implemented for sure.

4.2.1 Double layer

So far all types of thin-film sensors that have been seen in the literature are shaped like a serpentine. This form of sensor maximizes performance in terms of spatial resolution and resistance of the sensor [2]. In the Figure 2.4 you can see a good example of this type of sensor. The main advantage of this option is its simplicity when it comes to achieving different resistance by adding more or less length to the coil.

In this case, choosing that option would mean to externalize the manufacturing of the sensors. They are thin films made of Nickel (maximize thermal sensitivity) on a polymer substrate, KAPTON. Both the sensor and the wiring are included in the sheet entrusted to the company, this implies that the only thing that should be manufactured in the institute is the substrate of ceramic material for the subsequent adhesion of the sheet to it.

This offers simplicity for the VKI because the manufacture of the sensors would be avoided, it seems easier when applying it to curved surfaces (it would only be necessary to glue the already manufactured flexible sheet), but it implies a complex calibration and the presence of different materials, so it would be a double layer probe, for which there is only an analytical solution in case of step in heat flux. This means that the code for heat transfer and temperature calculations could not be validated.

In addition, as seen in [2], when the ceramic cylinder is very small, adjusting the sheet to such sharp curves is not a simple task. The sheet tends to break and peel off during the tests, thus introducing error in the measurements by the formation of air bubbles between the KAPTON layer and the substrate.

4.2.2 Single layer

On the other hand, there is the option to paint the sensor directly on the ceramic substrate. This option is less complex but requires more work by the institute's technician, since the VKI laboratory technician would also be responsible for manufacturing these sensors. This alternative is more robust, there is no risk of breaking the sensor or wiring.

The Figure 4.1 shows a vertical and horizontal example of what the technician is capable of doing on a 6mm diameter MACOR cylinder.

To control the resistance of this type of sensors the technician paints the first layer of Nickel/Platinum and bakes the probe so that the material settles. Once seated, he measures the resistance that said layer has and add more, repeating the process, until the desired resistance is obtained. It is a complex and laborious process.

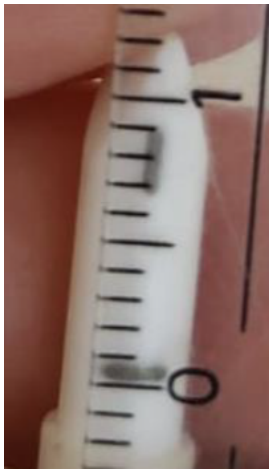

Figure 4.1: Thin films samples made by the VKI technician.

Due to all the problems that the double layer has been giving in the probes that have been manufactured until today, the option of only one layer is chosen for the design of the final probe. The sample is analyzed more accurately with the examples provided by the technician that can be seen in the Figure 4.1, and the main features are collected in the Table 4.1.

Material	Length [mm]	Width [mm]
Platinum	2.1	0.90

Table 4.1: Painted thin films characteristics.

4.3 Basic probe parameters

Once determined the dimensions and characteristics of the sensors that have been chosen, you can proceed with the design of the substrate, according to these dimensions. This dimensioning is going to be divided into three different parts since each one is limited by different requirements: length, diameter, and the hole for the heater placement.

Regarding the choice of the material of the said substrate, MACOR is chosen. It is a ceramic material that has already been used in the previous designs at the institute and whose properties are included in the Table 4.2

Material	$\rho\ [kg/m^3]$	$C_p\ [J/kg \cdot K]$	$k\ [W/m \cdot K]$
MACOR	2520	752	1.672

Table 4.2: MACOR thermal properties [2]

4.3.1 Length

The final length of the probe is defined by the number of sensors implemented, their width, the separation between them and the distances left between the first/last thin-film sensor and the tip/bottom of the probe. As will be seen later, the final length will vary for the latter reason after studies of the thermal behavior once the support has been added, but for the moment the part that would contain the sensors will be sized.

The total span length to be characterized is 70.3 mm. The ideal would be to cover that length with the smallest number of possible measures while maintaining a spatial resolution of approximately 1 mm. To determine the necessary characteristics that provide a balance between a feasible design and that fits the needs, several parametric studies are carried out with the help of an Excel sheet.

First of all, try to make a first approximation of the spatial resolution with which you want to scan the total span. It is considered that making measurements every 4% would be an acceptable resolution, this implies a maximum spatial resolution of 2.8 mm. It is much more than 1mm but it has to be considered that 1 millimeter means less than 1mm separation between thin-films. If cabling as to be added too after the sensors, this distance is too small: 1mm is not realistic. To cover the total length every 2.8 mm, a total of approxi-

mately 25 points is required.

A minimum distance of 1.6 and 5 mm between the last and first sensor and both ends of the probe is fixe. Taking these distances into account and the dimensions that the sensors will have according to the Table 4.1, a parametric study is carried out to find a balance between the number of sensors included in the probe and the number of total measurements to cover the length completely, computing the final probe length for each case.

After several studies, it is determined that the number of final sensors will be 9. In this way, with only 3 measurements it is possible to cover the entire length of the span. The final length that is computed with these characteristics is 30 mm. The Table 4.3 summarizes the parameters set after this point.

Resolution [mm]	**Sensors per probe**	**Upper min distance [mm]**	**Bottom min distance [mm]**	**Total probe length [mm]**
2.8	9	5.0	1.6	30.0

Table 4.3: Probe characteristics I

4.3.2 Diameter

As indicated in previous sections, one of the assumptions when performing the algorithm that computes the temperature is to assume the probe as a semi-infinite solid. That is, the conditions in the center of the probe will remain constant regardless of what happens on its surface.[3]

As indicated in the literature, in order to consider a solid of thickness 2L as semi-infinite, it is necessary for the Fourier number (Fo) to be less than or equal to 0.2 [3]. The Fourier number is a dimensionless number that characterizes transient heat conduction. Conceptually, it is the ratio of diffusive or conductive transport rate to the quantity storage rate[21]:

$$Fo = \frac{\alpha \cdot t}{L^2} \leq 0.2 \tag{4.1}$$

where *alpha* is the thermal diffusivity, t the duration of the test and L the half-distance between the stagnation point and the center of the probe or the

start of the heater hole. Substituting the corresponding values:

$$\alpha = 0.73mm^2/s$$

$$t = 0.7s$$

the minimum length that must be in order for the assumption of semi-infinite solid to be valid can be cleared and calculated, Equation 4.2

$$Fo = \frac{\alpha \cdot t}{L_{min}^2} = 0.2 \longrightarrow L_{min} = \sqrt{\frac{\alpha \cdot t}{0.2}} \longrightarrow L_{min} \approx 1.6 \tag{4.2}$$

Taking into account the result obtained, the minimum distance that should be considered would be $2L$, that is, approximately 3.2 mm.

In addition to the assumption of semi-infinite solid, it will also be verified that the thermal penetration depth ($delta_p$) is less than the previously calculated distance.

According to [3], la thermal penetration depth is the depth to which significant temperature effects propagate within a medium. It can be fixed, for example, as the x location at which $(T - T_s)/(T_i - T_s) = 0.9$. Being T the temperature at position x, T_s the temperature at the surface and T_i the inner temperature.

Considering the case for constant surface temperature:

$$T(0, t) = T_s$$

The temperature ratio can be defined as:

$$\frac{T(x, t) - T_s}{T_i - T_s} = erf\left(\frac{x}{2\sqrt{\alpha \cdot t}}\right) \tag{4.3}$$

where, again, α is the thermal difussivity and t the test time. $erf(w)$ is the Gaussian error function [3] defined as:

$$erf(w) = \frac{2}{\pi}\int_0^w e^{-v^2} dv \tag{4.4}$$

and tabulated in the Appendix B of [3].

The table founded on that appendix is introduced in Matlab to compute the different values of thermal penetration depth for each possible temperature ratio. Figure 4.2 shows the results obtained with that script.

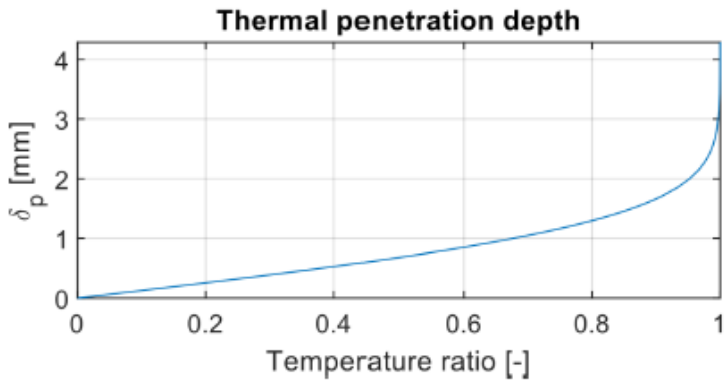

Figure 4.2: Thermal penetration depth.

As it can be seen in Figure 4.2 for thermal penetration depth values above 3mm the temperature ratio is almost 1. This means that the diameter of the MACOR substrate could be fixed at 3mm. So the final diameter for the probe is going to be 6mm.

4.3.3 Heater hole

Once the dimensions of the substrate have been defined, the problem arises of making the hole for the heater. It must be taken into account that it will be a very small hole inside a ceramic cylinder, and therefore fragile, which should also cover the total length of the probe so that the final temperature of the probe is as homogeneous as possible.

The first option, also made in [6], is to make a concentric hole between 1.5 and 2 mm in diameter. The problem with this solution is that, this way, the distance established in the two previous subsections in order to fulfill the assumptions of semi-infinite solid would no longer be adequate.

In [2] it was proposed to decentralize the hole for the heater. This was also manufactured in the institute laboratories, so it is supposed to be a feasible solution. The Figure 4.3 shows the 2D scheme of how a transverse section of

the probe would be, with a final diameter of 6mm, hole of 2mm diameter for the heater and a distance between the centers of 1.25mm, leaving 3.25 mm distance between the probe surface and the start of the heater hole. In the next sections the penetration depth will be studied in COMSOL in order to validate this results.

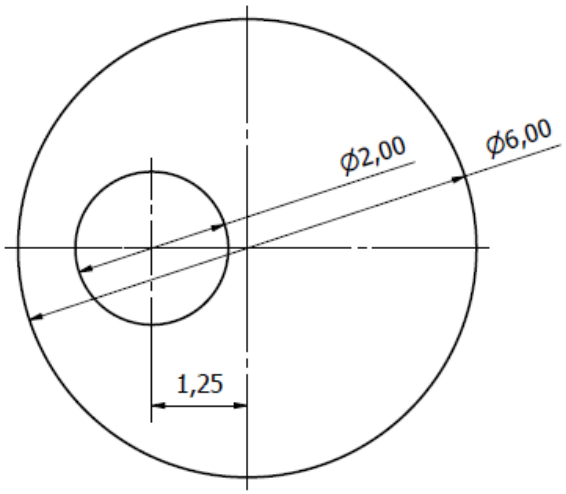

Figure 4.3: 2D Probe scheme.

The heater will consist of a coiled wire so that the heat flux and power it will provide will be due to its joule heating. The number of loops and dimensions of the heater must be determined to cover the entire length of the probe. A small parametric study is carried out to know in advance the general characteristics of the heater: dimensions and power that will generate given a certain voltage. The study will be based on the temperature increase achieved with these characteristics.

On the one hand, the heat flux that the heater will provide is calculated based on its main characteristics: total resistance. This resistance depends on the total length of the coiled wire and its resistance per meter. The total cable length will depend on the number of loops that are made, and this will determine the minimum length of the heater.

Once the total resistance of the heater has been determined, its power can be determined as:

$$P = \frac{V^2}{R_{heater}} \tag{4.5}$$

Now, starting from the scheme shown in the Figure 4.4. The heat flow q is imposed by the heater. The values of the thermal coefficients k and h are known, as well as the area A and length L. The only unknown parameter is then the temperature gradient:

$$\Delta T = q \cdot \sum R = q \cdot \left(\frac{L}{k \cdot A} + \frac{1}{h \cdot A} \right) \tag{4.6}$$

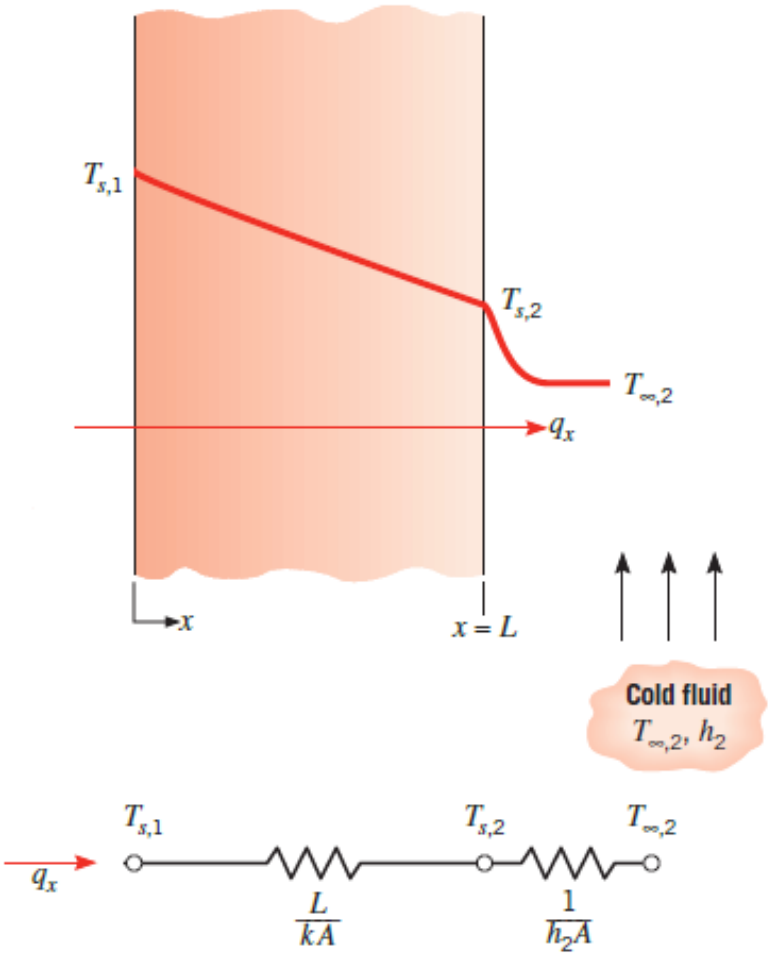

Figure 4.4: Heat flux scheme for the MACOR substrate [3].

An excel sheet with all the parameters has been developed to be able to directly obtain the temperature gradients according to all the parameters. After several parametric studies, it is considered that it is possible to achieve final temperatures of 360 K with a heater that provides a power of 1060 W/m^2. To reach this power, 100 loops are needed around a cylinder approximately 2 mm in diameter with a cable whose resistance is 21.32 Ohm/m, implying

a minimum length of 25 mm. For longer heaters the only thing that should change is the distance between loops.

4.4 Yaw angle sensitivity

The probe must be prepared to measure in highly three-dimensional flows, that is, the sensitivity at yaw angles of the flow should be as low as possible. Therefore, the position of the sensors along the ceramic substrate is very important.

For a first approximation of where the thin films can be positioned, we start from the bibliographical study on the characteristics of the flow around a cylinder.

Then, the optimal position of the probe with respect to the flow and the different measurement options are studied using the actual yaw angles present in a test as a basis.

4.4.1 Flow characteristics around the cylinder

The first step is to know the characteristics of the flow around the cylinder in terms of Reynolds number, pressure, temperature, and Nusselt number.

Reynolds number

The Reynolds number is a dimensionless number that determines the importance of inertial forces against vicious forces. Therefore it is also an indicator of the type of flow: laminar or turbulent.

The study of the Reynolds number is carried out, as said before, due to its great influence on the fluid's behavior. When the Reynolds numbers are low, the viscous effects predominate and therefore, the flow remains adhered to the surface of the cylinder. On the other hand, as Reynolds number increases, the inertial effects become more important, thus affecting the behavior especially of the wake and detachment point of the laminar layer.

A more detailed study on the evolution of the flow behavior around the cylinder as the Reynolds number increases can be found in [10]. In this bulletin, it can be seen how initially for Reynolds under 5 there is a regime of unseparated flow. Up to $Re = 40$ values are already appearing to a fixed pair of vortex in the wake. From Reynolds values from 40 to 150 two different regimes in which vortex street is laminar can be found: a periodicity governed in low Re range by wake instability and/or periodicity governed in high Re range by vortex shedding. After $Re = 150$ till $Re = 3 \cdot 10^5$, which is the type of flow regime where the test are carried out, there is a transition range to turbulence in vortex that, once Reynolds numbers of 300 or more are reached, ends up as a vortex street fully turbulent [10]. Figure 4.5 shows a scheme of the flow characteristics under this range of Reynolds number, this is flow profile that should be expected during test conditions.

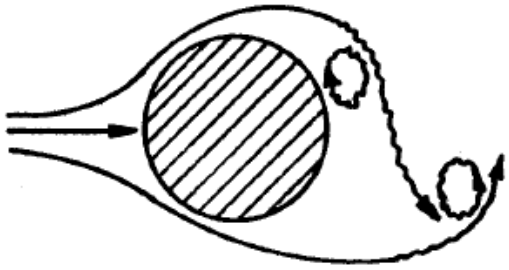

Figure 4.5: Flow configuration around a cylinder for Re numbers between 300 and $3 \cdot 10^5$ [10].

Now, looking at Figure 4.5 is easy to deduce that the next important step is to know at what angle of attack the flow is detached from the cylinder surface, in order to avoid painting the sensors above that angle. A CFD study was carried out by M. Bassignana in [2]. According his study the flow separation for Reynlods numbers around $1.3 \cdot 10^4$ (test conditions) occurs at 82 degrees. Therefore, the thin-film sensors should not cover more than ± 80 degrees[1].

Presion

Studying the pressure coefficient the point at which the flow is detached from the cylinder surface can be determined too . In [2] a comparative study of the potential theory with other experimental cases carried out in [15, 16]

[1] This is without considering all the parameters yet.

determine that the separation point is around 70 degrees.

Temperature

The final goal is to determine the flow total temperature, which corresponds with the adiabatic wall temperature at the stagnation point. The possibility of some temperature recovery once the flow advances along the cylinder surface should be taken into account. If the temperature varies greatly after a certain distance is advanced, that distance should be considered to reduce the sensor length until it falls within an acceptable temperature gradient range.

For the flow recovery temperature and wall temperature the work found in [4] is used. The flow evolution from the stagnation point can be considered as an isentropic acceleration, therefore the recovery temperature can be studied for different Mach numbers. Figure 4.6 shows the results obtained for different Mach numbers, even for the limiting case of hypersonic flow ($M \longrightarrow \infty$).

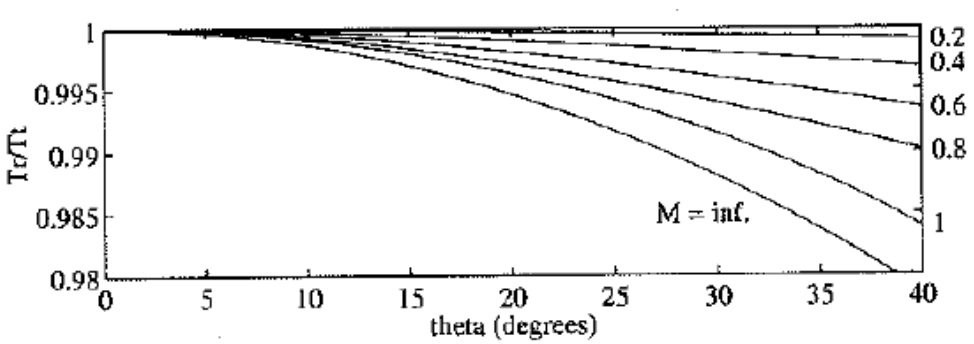

Figure 4.6: Flow recovery temperature around a cylinder for different Mach numbers [4]

As it can be seen in the previous figure, the variation of the flow total temperature due to the isentropic acceleration is not relevant.

Nusselt distribution

This last parameter is important since it is a dimensionless number that measures the increase in heat transmission from a surface by convection compared to the heat transfer that would occur if only conduction existed [22]. Therefore large changes of the said number along the surface of the cylinder would induce errors in the measurements if the sensors were located in that

area.

There is no (or not found) analytical solution that shows the values of this dimensionless number along a cylinder under certain flow conditions. All studies are experimental, empirical or numerical [11, 17].

M. Bassignana compares and contemplates the solutions obtained for Reynolds numbers equal to $1.3 \cdot 10^4$ comparing the empirical formula proposed by G.W. Lowery in [11] with interpolation from the experimental data by Schmidth in [17].

To simplify the process, the decisions that involve taking into account the number of Nusselt are based on the Figure 4.7 found in [17]. This figure summarizes the different distributions of Nusselt numbers for different Reynolds numbers around a cylinder.

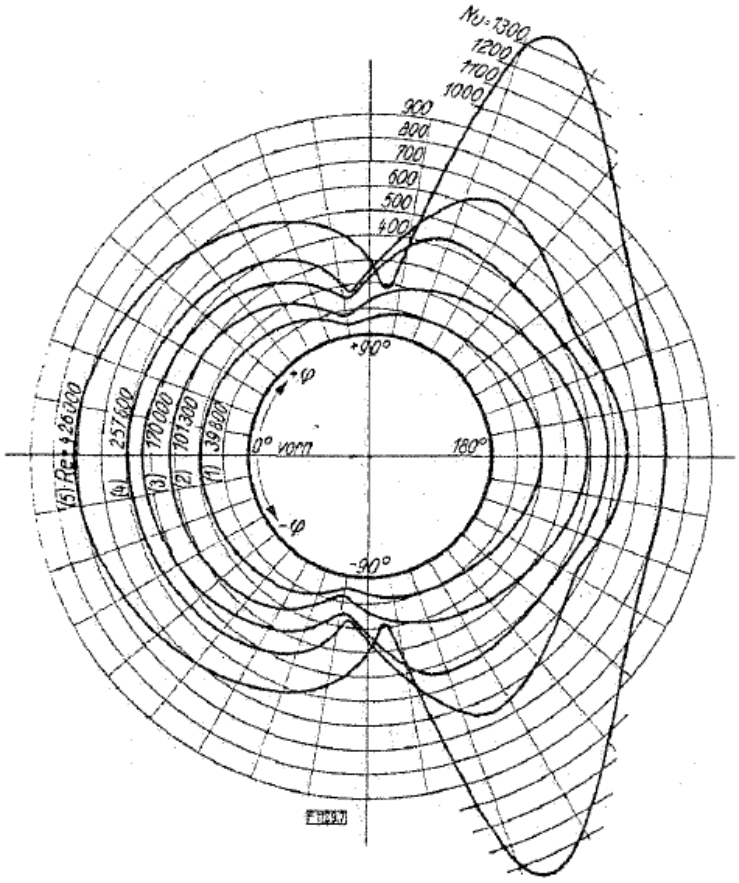

Figure 4.7: Nusselt distribution around a cylinder for different Re numbers [17]

Considering Figure 4.7, for low Nusselt numbers variations the angle considered should be, at least, less than 30 degrees. This statement is more in line with the sensors found in the literature and the angles they covered from the stagnation point. In almost all items found it is recommended that the sensor should not cover more than $\pm 20 - 25$ degrees[4].

Thus, the number of Nusselt remains as the most restrictive and therefore decisive parameter when establishing the angle occupied by the sensor and, therefore, the final length of the thin film sensors. Given that the diameter of the probe is 6 mm and the angle α limit is $20 - 25$ degrees, the maximum length of the sensors will be 2.62 mm:

$$\frac{d \cdot \pi \cdot 2\alpha}{360} = \frac{6 \cdot \pi \cdot 2 \cdot 25}{360} = 2.62mm \tag{4.7}$$

According to the **??**, the institute's technician is able to paint sensors that are only 2.1 mm long and 0.9 wide. Thus, these dimensions that could be taken into account from now on for future calculations and studies.

4.4.2 Test yaw angles profiles

After studying the behavior of the flow around a cylinder and establishing the margin angles between which the sensors should be placed to measure with the least possible error, the possible positions or configurations of the probe for the actual yaw angles studied and measured at the CT3 facility.

From the recovery temperature equation, assumed isentropic acceleration and a variation of the static pressure near the stagnation point using a Newtonian approximation [4, 2], the error due to misalignment of the probe for different sensorlengths can be calculated. The Figure 4.8 shows the evolution of this error.

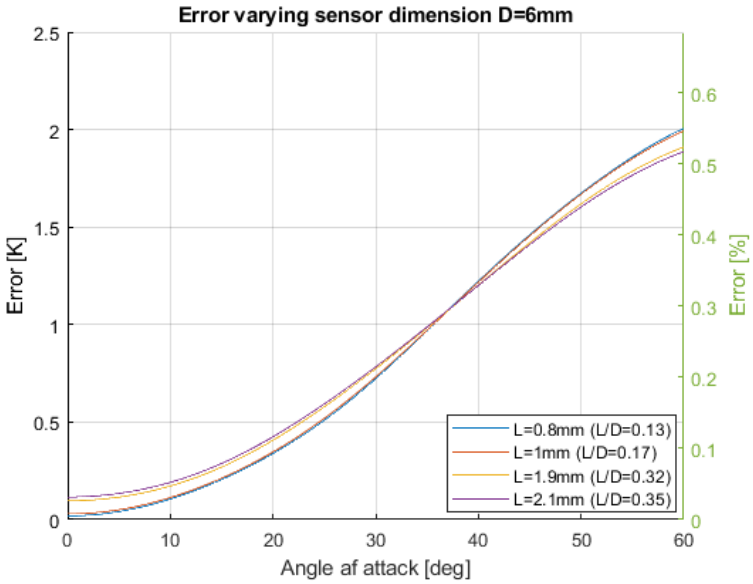

Figure 4.8: Error due to flow misalignment for different sensor lengths.

If an error of less than 1K is to be set, as specified in the design requirements, the sensor should not be more than 30 degrees relative to the flow. As can be seen in the autoref fig: matlab the length of the sensor at the end is not so decisive, as long as the probe is aligned with the flow. Of course, the fact that the sensor is smaller helps that it does not cover so much section of the cylinder and it is easier for the seen angle with respect to the flow to be smaller.

The next step is to iterate the design of the probe to be able to sweep the total span length with the least possible number of measurements, being able to change the angular orientation of the probe in each of these measurements, thus adjusting the maximum and minimum yaw angles that you could see the probe in the different positions.

The Table 4.4 includes the different options contemplated.

	Option 1	**Option 2**	**Option 3**	**Ideal**
Probe length [mm]	36.3	24.3	25.3	26.7
Sensors per probe	12	8	12	14
Spatial resolution [mm]	3	3	2	1.8
Sensors separation [mm]	2.2	2.2	1.2	1
Measurements needed	2 (+1)	3	3	3

Table 4.4: Probe configurations for improving yaw angles sensitivity.

The Figure 4.9 schematically shows how the different measures would be: the percentage of span they would cover and the maximum yaw angles that

take place. As it can be seen, the most critical part is the last 20% of the span.

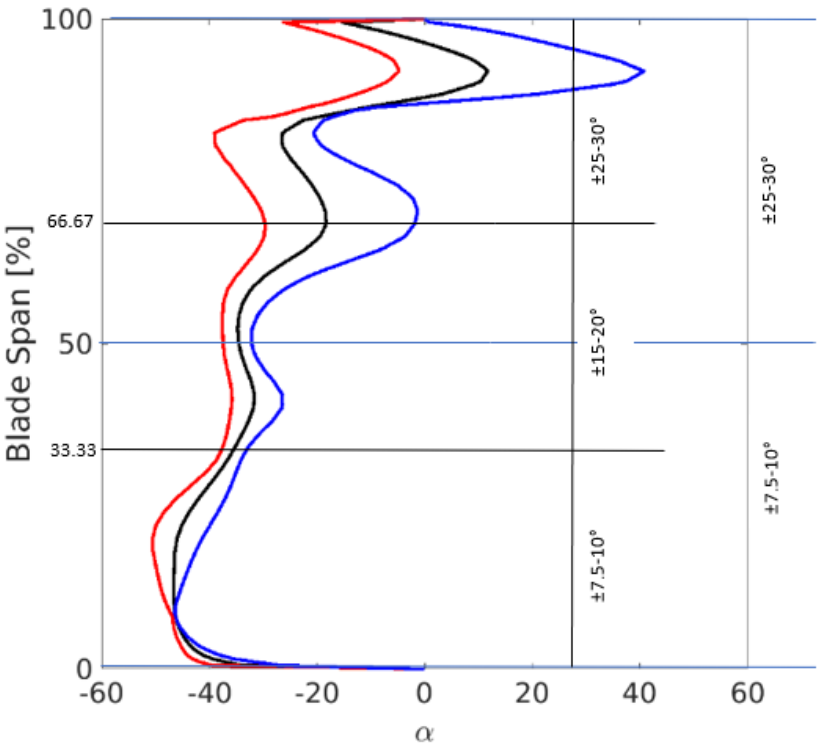

Figure 4.9: Measurements division and maximum yaw angles for each section.

As the Table 4.4 summarizes, all three options need 3 measures. In the case of option 1 the third measurement would be performed in the second half of the total span again, but reorienting the probe to be able to better capture the last points. In addition to complex and tedious, a much longer probe is necessary. This option is the first to be discarded. Comparing options 2 and 3 with the Ideal and trying to create a balance, option 2 is finally chosen. Option 3 seems much better because it does not require much more probe length and the spatial resolution is better, but you have to take into account that introducing 12 sensors in such a small space is very complicated. In this case, it would be practically impossible to configure the wiring of 12 sensors in such a small space. Therefore, option 2 is, in the end, the one chosen to carry out the measures.

The next step is to know the angles to which each measure should be oriented to reduce the yaw angle (α) and, with it, the error due to flow dealignment. The Figure 4.10 shows an outline of what is determined as angle α.

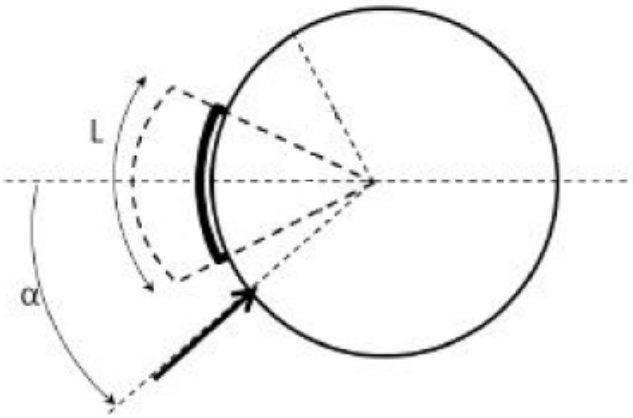

Figure 4.10: Scheme of the probe: yaw angle and sensor length [2].

% total span	Test values [deg]			Per 1 t-f [deg]	Per 9 t-f [deg]	Final yaw angles [deg]			
	Min	**Main**	**Max**	**Mean**	**Mean**	**Min**	**Main**	**Max**	**Mean**
99,79	-25	-15	0	-16,83		7	-3	-18	-1,17
95,80	-10	3	28	-17,25		-8	-21	-46	-0,75
91,82	-6	10	38	-22,95		-12	-28	-56	4,95
87,84	-16	-5	5	-10,10	17.57	-2	-13	-23	-7,90
83,85	-37	-25	-20	-28,25	∼	19	7	2	10,25
79,87	-38	-25	-18	-28,24	18	20	7	0	10,24
75,89	-35	-22	-7	-24,21		17	4	-11	6,21
71,91	-31	-19	-3	-21,06		13	1	-15	-3
67,92	-30	-18	-2,5	-20,25		12	0	-15,5	-21
63,94	-33	-25	-11	-24,73		1	-7	-12	-28
59,96	-35	-30	-24	-30,01		3	-2	-2	-13
55,97	-37	-33	-30	-33,46		5	1	19	7
51,99	-37	-35	-33	-35,04	32.48	5	3	20	7
48,01	-37	-34	-31	-34,09	∼	5	2	17	4
44,03	-36	-32	-27	-31,88	32	4	0	13	1
40,04	-35	-32	-26	-31,22		3	0	12	0
36,06	-37	-34	-31	-34,09		5	2	-1	2,09
32,08	-38	-36	-34	-36,04		6	4	2	4,04
28,09	-42	-40	-35	-39,11		-2	-4	-9	-4,89
24,11	-48	-44	-38	-43,53		4	0	-6	-0,47
20,13	-50	-45	-41	-45,48		6	1	-3	1,48
16,15	-50	-46	-43	-46,42	43.80	6	2	-1	2,42
12,16	-49	-47	-45	-47,03	∼	5	3	1	3,03
8,18	-48	-47	-47	-47,34	44	4	3	3	3,34
4,20	-46	-45	-44	-45,01		2	1	0	1,01
0,21	-40	-35	-30	-35,24		-4	-9	-14	-8,76

Table 4.5: Excel yaw angles study for probe positioning.

A study is carried out in Excel, where the values of the main, minimum and maximum yaw angles are entered for 26 different points divided equally along the total span. From these three values, the average yaw angle that every sensor would see at each of the points is calculated. The values are grouped into groups of 9 points (number of total sensors present in the probe and thus, total number of points per measurement) and the quadratic mean of those 9 points is calculated. The resulting value gives us an idea of the angle at which the probe should be placed to achieve the best results.

The values obtained are collected in the Table 4.5. The last three columns record the main, minimum and maximum angles that each sensor would see with the probe already positioned at the correct angle, as well as the mean angle. As expected, the only critical points are above 90% of the total span. In this last section the angles vary very quickly, it is very difficult to align the probe so that all the sensors work under conditions close to the ideal ones. In terms of mean angles the values are acceptable, so it is determined that the final configuration will be: a 9-sensor probe with which measurements will be made in 3 different positions, the first at 44 degrees, the second at 32 and the third to 18.

4.5 Cabling

Another point to consider is the wiring, necessary to power the sensors with certain electrical currents and to extract the necessary information to later calculate the heat fluxes and temperatures.

It is not possible to weld directly a cable to the sensor, so the option of painting gold tracks from the ends of the sensors to the rear of the probe is chosen. The main problem of this method is that it is necessary for the surface on which it is painted having no discontinuities or edges, therefore it will be necessary to ensure that this condition is met.

Once the gold trucks have been painted, it is possible to weld wires to the golden paths. This welding must be carried out on the back of the probe, where it will be necessary to size a slot or space to be able to store the cables. By finally having nine sensors, it will be necessary to size this space for a total of eighteen cables, two per sensor. Taking into account that these cables

have a diameter of 0.2 millimeters a total cross-sectional area of 0.57 square millimeters is necessary to be able to introduce all the cables. A final area of 1 square millimeter is established to simplify and keep a certain safety margin.

The initial idea was to make a rectangular slot in which to introduce the cables to be able to take them outside. The scheme of this slot can be seen in the Figure 4.11. Obviously space is insufficient, in addition, the welding has to be performed on a flat surface, it is impossible to paint the gold wires inside of the slot since there are edges and discontinuities.

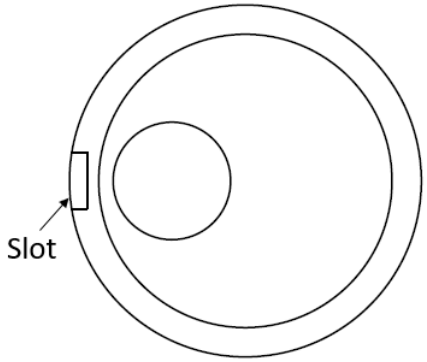

Figure 4.11: Slot scheme.

Therefore, it is decided to make a notch that leaves a flat surface at the back of the probe, filing the edges so that there is a smooth transition between the curved surface and the surface for welding the cables. To know how far the notch should be made, the area of the circular segment that covers the surface necessary to store all the cables is studied.

$$Area = \frac{1}{2} \cdot r^2 \cdot (\alpha - sin(\alpha)) \tag{4.8}$$

where r is the probe ratio and α the covered angle.

To calculate the depth of the notch h that implies a certain angle:

$$h = r \cdot (1 - cos(\alpha/2)) \tag{4.9}$$

The parameter to be determined is then α, from which h will also be determined. The important thing is that the depth of the notch is not larger than the distance between the surface of the probe and the heater: 0.75 mm. The Figure 4.12 shows the different angles and the areas that are achieved for each case.

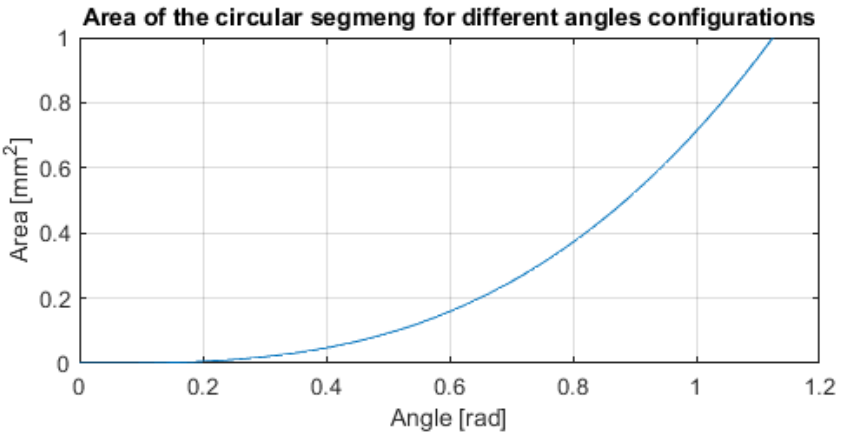

Figure 4.12: Cabling slot areas computed for different angles.

With an angle of 1,125 radians, or what is the same, 64.46 degrees, an area of 1 square millimeter and notch depth of 0.46 millimeters is achieved. To calculate the resulting circumference segment's cord with these values:

$$c = 2 \cdot r \cdot sin(\alpha/2) \approx 3.2mm \tag{4.10}$$

In this way, the space for the cables is characterized and sized. The total area available to weld the cables will be a rectangle of base c and height equal to that of the probe. An outline of the current slot is shown in Figure 4.13. As indicated above, it is necessary to file the edges that occur with the joint of the slot and the surface of the cylinder to be able to paint the gold wires without problems.

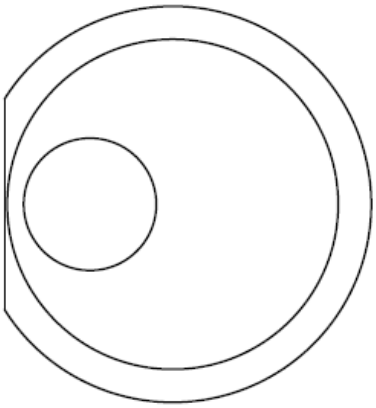

Figure 4.13: Final slot scheme.

Once all the cables are welded, the entire area will be covered with a special glue available in the VKI laboratories, molded and polished to obtain a

smooth and circular final surface, as if the slot did not exist.

It must be taken into account that the slot must also be made at the beginning of the support, in order to take all the cables out.

4.6 Thin films Joule heating

A factor that until now has not been considered is the heat flux produced by the Joule heating of the sensors. This point is important to keep in mind because it can affect the final temperature of the substrate if the values are very high. To solve this problem a small calculation is made for the different currents that can be found in heat transfer signal conditioning [2]. The formula that provides power dissipated by the joule effect is:

$$E = R^2 \cdot I \tag{4.11}$$

where R is the resistance of the sensor and I the electrical current that will fed the sensors.

As we want to obtain the heat flow, it is necessary to divide by the surface occupied by the sensor. Taking into account that the dimensions set for the sensors are 2.1 millimeters in length and 0.9 millimeters in width, the values obtained for different resistance and electrical current values are included in the Table 4.6.

Heat flux $[W/m^2]$			
Resistances	**Amperage**		
[Ω]	**5 [mA]**	**10 [mA]**	**15 [mA]**
25	331	1323	2976
50	661	2646	5952
75	992	3968	8929

Table 4.6: Heat fluxes computed for different thin-film joule heating.

The heat fluxes obtained can become very high in cases of greater resistance and amperage. It is recommended to minimize both the resistance of the sensors and the current with which they are fed so that joule heating affects as little as possible the measurements and the final temperature of the substrate. The most important part of this issue is trying to keep the sensors from affecting each other. But taking into account that the current will be

passed through the sensors just before the test begins, there will be virtually no time for the sensors to warm up or affect each other, since once the valve opens and the flow is released the convection coefficient increases dramatically.

4.7 COMSOL 2D design

Once the design of the probe and the characteristics of the sensors have been set, the thermal behavior of the probe is studied. For this, the COMSOL Multiphysics software that has been introduced in the section 3.2 is used. The study is mainly divided into studies in two and three dimensions. Next, the most relevant ones carried out in 2D will be shown. For this case the cases are divided into static and transient studies.

4.7.1 Static

These studies have been carried out, above all, to know the distribution of temperatures in the substrate under different conditions. The first study is to verify if the calculations made with the excel sheet in subsection 4.3.3 are correct and the final temperature reached in the substrate is homogeneous and equal to the estimated in the analytical calculations, as well as knowing the temperature contours.

Las condiciones de contorno fijadas son: flujo convectivo alrededor de la sonda con un coeficiente de convección $h = 5W/m^2K$ y un flujo de calor impuesto en las paredes del agujero del heater de $q = 1060W/m^2$. El mallado que se realiza es automático y con un tamaño medianamente pequeño ya que el estudio es muy sencillo y no necesitamos una gran precisión.

The boundary conditions are: convective flow around the probe with a convection coefficient $h = 5W/m^2K$ and a heat flow imposed on the heater hole walls of $q = 1060W/m^2$. The meshing that is done is automatic and with a moderately small size since the study is very simple and we do not need great precision.

The Figure 4.14 shows the temperature distribution along the probe assuming a heat flow provided by the heater of 1060 W/m^2. According to the

excel sheet, the temperature value at the stagnation point should be 360K. As can be seen, the temperature reached according to COMSOL is 4K higher, so it can be determined that for a first approximation the excel sheet is valid.

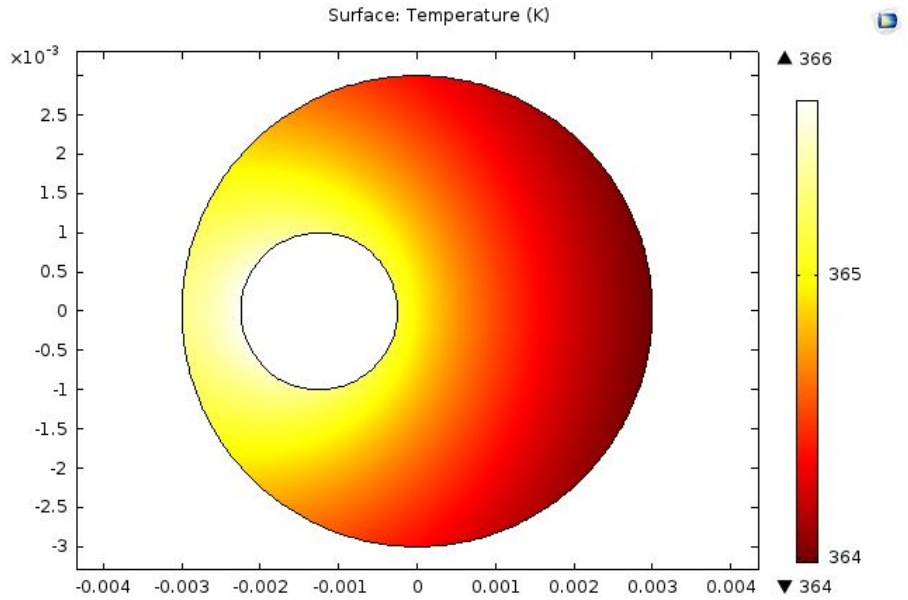

Figure 4.14: Temperature distribution with a heat flux imposed of 1060 W/m^2.

The next and last two-dimensional static study is a parametric study of how joule heating of the sensors can affect the final substrate temperature. Six different heat flows are imposed corresponding to the first two columns of the Table 4.6.

The Table 4.7 collects the approximate temperatures obtained at the stagnation point for the different heat flows imposed:

Resistance [Ω]	**Amperage [mA]**	**Heat flux [W/m^2]**	**Temperature**
0	0	0	364
25	5	331	372
50	5	661	379
75	5	992	387
25	10	1323	395
50	10	2646	425
75	10	3968	456

Table 4.7: Temperatures reached at the stagnation point after imposing a heater heat flux of 1060 W/m^2 and different thin-film joule heating options.

It can be seen that, as expected, one should seek to have sensors with the lowest possible resistance and feed them with the smallest current. For

the limit cases of higher current and resistance the heat flux produced is very high. What can be observed when viewing the evolution of the temperature distribution as the heat flux is increased due to the Joule heating effect is that, above all, the most important thing is that the flow caused by the sensor should be less to that provided by the heater, or much larger.

The Figure 4.15 collects the temperature distributions ordered from left to right, the first one with an imposed flow along the sensor of 0 W/m^2 and the last one corresponding to a flow of 1323 W/m^2. As can be seen, as the heat flux imposed by the heating of the sensor approaches the value of the one established for the heater, it is more difficult for the entire sensor to be at the same temperature. That is, homogeneous temperature distribution along with the sensor in the case where the joule heating is much greater than that provided by the heater, the sensor will have a homogeneous temperature again, but its high temperature will produce lateral conduction and could affect the thin films around it more.

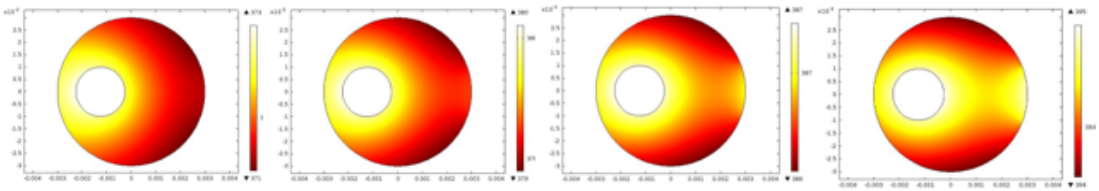

Figure 4.15: Evolution of the temperature distribution after increasing the heat flux produced by the sensor.

In short, the static behavior of the ceramic substrate is as expected. It is recommended to maintain resistance and amperage as low as possible to avoid the Joule heating effect and increase the power of the heater.

4.7.2 Transient

This study seeks, again, the characterization of the temperature contours of the ceramic substrate under conditions that simulate what will happen in the experimental tests.

Considering the operation of the facilities explained in section 3.1, the same conditions can be simulated by imposing the variation of temperature and con-

vection coefficient over the time and surface of the probe.

Initially, the probe is in almost vacuum conditions, so the convection coefficient is $h = 5\ W/m \cdot K$ and the temperature equal to the environment, $297\ K$. When the valve opens, a temperature peak is reached, which then decreases and tends to a constant value. As for the convection coefficient, it increases dramatically and remains constant throughout all the duration of the test, and then returns to its initial value. The Figure 4.16a and Figure 4.16b show the evolution of temperature and convection coefficient during the 0.7 seconds of the experimental test. These conditions are imposed within COMSOL as Matlab functions thanks to the module that allows both programs to be connected: Matlab LiveLink.

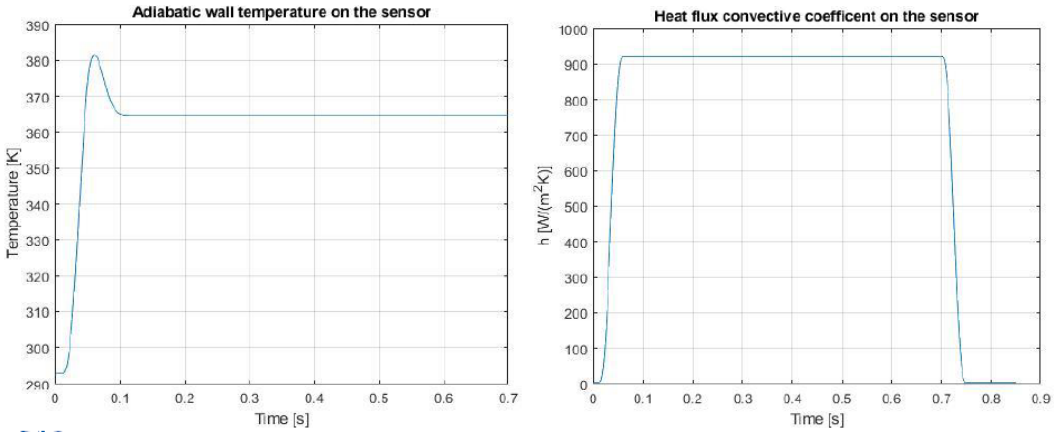

(a) Adiabatic wall temperature. (b) Convective heat flux coefficient.

Figure 4.16: Imposed evolution of the values on the sensor surface for the transient studies.

Under these conditions, it is expected that the temperature of the cylinder surface will decrease rapidly in the first 0.1 seconds and then continue to decline, but more gradually. The final temperature profiles indicate that the highest temperatures are at the center of the probe while the cylinder surface has a lower and homogeneous temperature due to the high convection coefficient (Figure 4.17 [2]).

[2]The diameter of this simulation is 5mm because corresponds to a study prior to the iteration of penetration depth

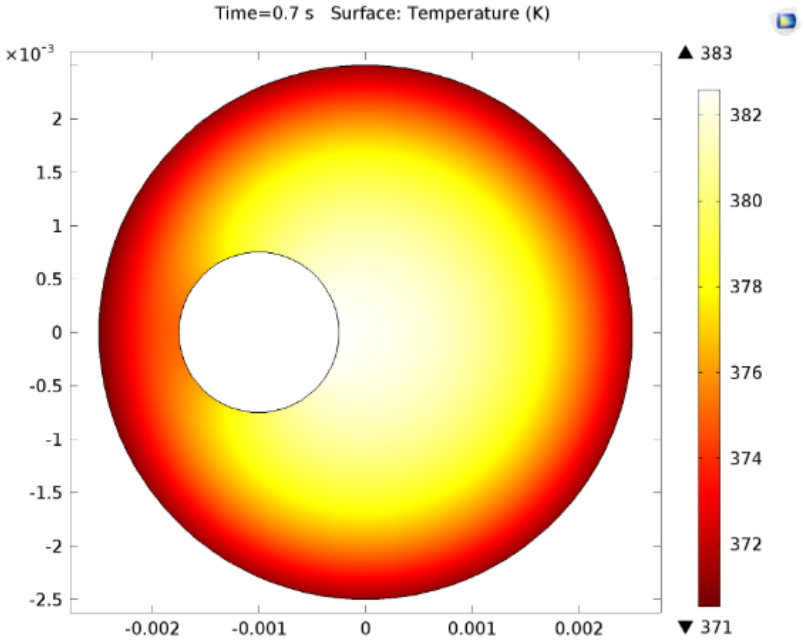

Figure 4.17: Temperature contours at the end of the test.

In addition to thermal characterization under test conditions, this simulation has been used to check the penetration depth. The evolution of the temperature is observed and plotted along a line that joins the stagnation point with the end of the probe, passing through the center of it. The results are shown in the Figure 4.18.

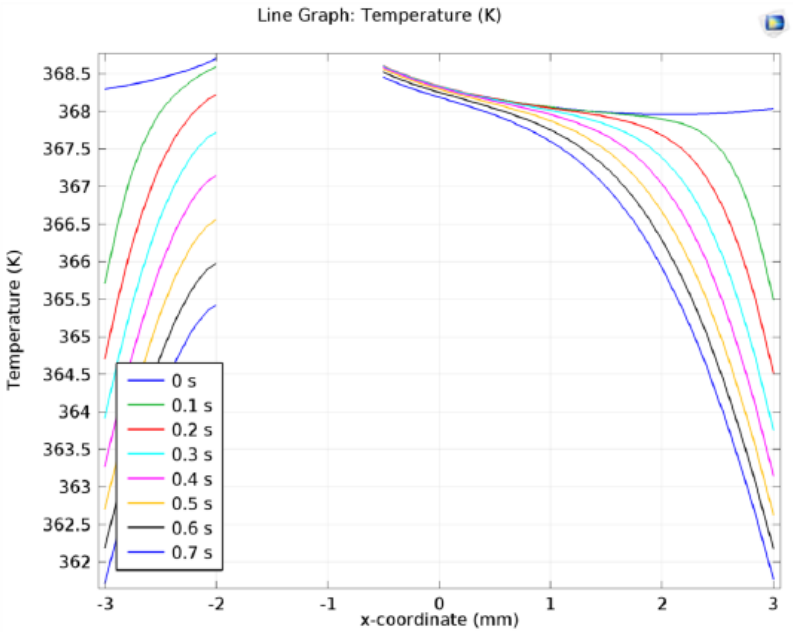

Figure 4.18: Temperature profiles along a line that joins the stagnation point with the back of the probe.

After observing the Figure 4.18 it is shown that in the center of the probe the thermal conditions remain constant despite the fact that the surface conditions vary. That is, modeling the probe as a semi-infinite solid is correct.

4.8 COMSOL 3D design

Once the studies in two dimensions are finished, we proceed with the third dimension. In this case, there are no transitory studies because the computational cost was very high and the simulations were very slow.

The purpose of this section is the same as the previous ones: the thermal characterization of the probe. It starts from the initial study of the probe itself, only taking into account the ceramic substrate. Then the support that is necessary to carry out the measurements is added, the possibility of different materials and the effect on the distribution of temperatures by adding another element is studied. Finally, the option of adding some type of thermal insulation between the ceramic cylinder and the support is raised.

4.8.1 Probe tip

The first step is the generation of the geometry in COMSOL, being only the part of the ceramic probe made with MACOR the process is simple. A cylinder of the dimensions indicated in Table 4.3 is created. After that, a hole that corresponds to the position of the heater is made. The boundary conditions are the same as those established for the 2D case: natural convection on the entire outer surface of the probe and a heat flux imposed that simulates the heat released by the heater.

The results obtained can be seen in the Figure 4.19. The highest temperature is 3K lower than that obtained in the 2D case. This may be due to the three-dimensional effects and the fact that the heater has been modeled as a non-through hole where only the side walls transmit heat. Therefore some leakage should be expected.

Despite this, the temperature distribution is as expected: the highest temperatures are near the heater and at the top of the probe, where the support

will be attached. This is because convection has been imposed only at the bottom of the probe. The temperature gradient generated between both ends is 6K.

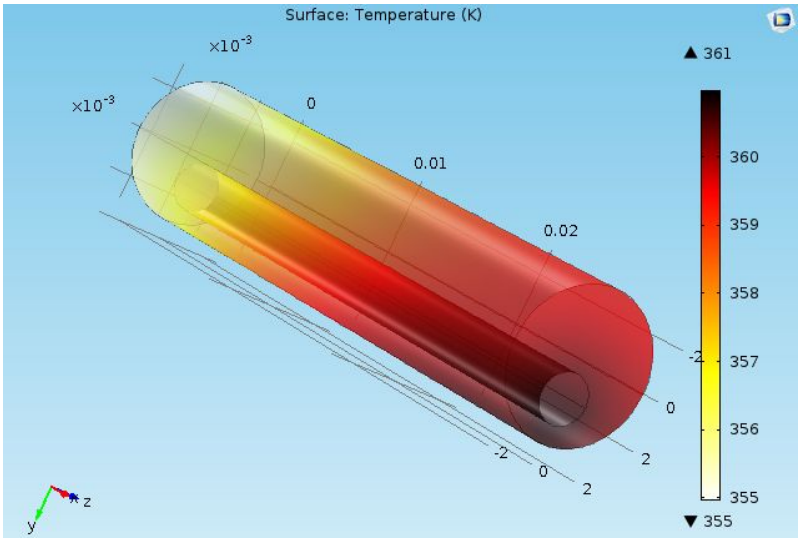

Figure 4.19: Temperature contours for the 3D MACOR substrate.

Studies were conducted for different depths of the heater hole. The deeper the hole, the better, since it ensures that the temperature gradient between ends is smaller and, therefore, the sensors are at less distinct temperatures. A total depth of 29 millimeters is set for the heater, that is, only 1 millimeter is left between the end of the ceramic substrate and the start of the heater. This way the heater is 0.5 millimeters below the last sensor, thus trying to ensure a more uniform temperature distribution.

4.8.2 Support

The previous study is useful to create a preliminary idea of the behavior of the substrate, but it must be taken into account that under real conditions, said substrate will be attached to a support made of another material: probably aluminum or brass. Therefore, the next step is to add this support and observe the effects it has on the thermal behavior of the probe.

The first problem that arises is the attachment of the probe to the support. To make the assembly easier, a part is added to the ceramic cylinder, also made of MACOR (all one piece). This part has a slightly smaller diameter that fits the inner diameter of the support and allows a simpler assembly with it. That

part will be inserted into the aluminum/brass cylinder. The Figure 4.20 shows a schema made with Inventor of how the new geometry of the ceramic probe would look. The possible influence of the length of this new part will be studied later, at the moment a height of 5 millimeters is established. Keep in mind that the hole for the heater must also pass through this part. This implies a longer hole and greater complexity for future manufacturing.

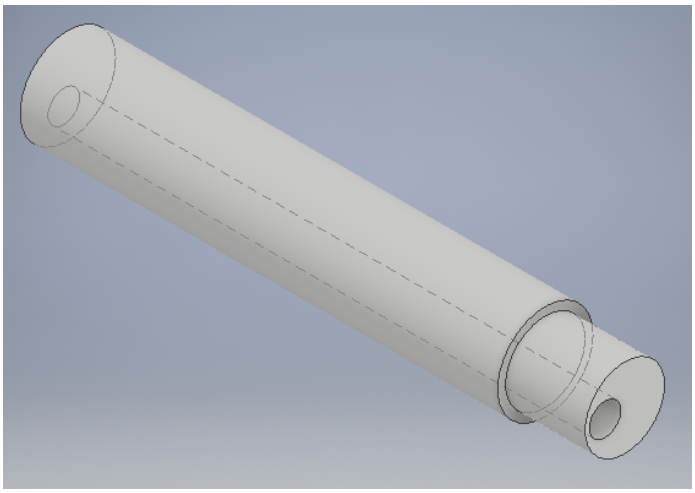

Figure 4.20: New MACOR substrate probe design.

The length of the support is determined by the total distance to be covered with the support and the probe, that is, from the very top of the stem to the bottom of the head (that basically touches the hub): 285 millimeters. This implies that if we have a 30 millimeters probe, the support should be 255 mm. The diameter is limited by the characteristics of the material available at the institute. In [6] it can be seen how the support was made with an eight mm diameter Brass.

Executing exactly the same case as before but with the added support, the maximum temperature reached is 332K, while before it was 361K. The main cause of the temperature difference is the losses caused by leakage towards the support. This implies that the power supplied by the heater must be changed in order to reach the desired temperatures.

The Figure 4.21 shows the temperature map obtained in the plane transverse to the probe just in the central part that divided both the probe and the support into two exactly symmetrical parts. This plane is the one that also contains the stagnation points.

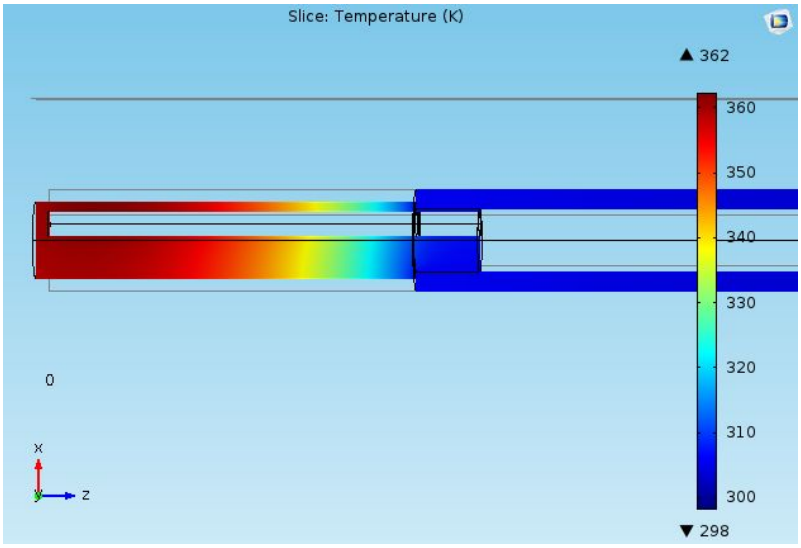

Figure 4.21: Temperatures map for an attachment of 5mm and Brass support.

As can be seen, the support is at the lowest and practically uniform temperature. The main temperature changes occur in the second half of the tip of the ceramic probe. A large part of the sensors are found in this area, this implies that the temperature gradients between the lower and higher temperature sensors are very high.

First, the influence of attachment length will be studied. As it has been indicated before, adding length that later has to be drilled implies a greater complexity at the time of manufacturing the probe. We must find a balance between a length large enough to provide robustness to the design and assembly but without adding too much complexity to manufacturing.

Another parametric study is carried out for three different attachment lengths: 5, 10 and 15 millimeters. The influence on the distribution of temperatures is practically imperceptible. The maximum temperature reached for the case of greater length (15 millimeters) is 1 K higher, but this is because the heater is resized so that its dimensions coincide all the time with the total length of the hole made in the ceramic part. A final length of 10 millimeters is chosen as it is the intermediate solution, it does not add much complexity to the manufacturing and it helps make the assembly a little more robust.

The possibility of using different materials is also studied: brass or aluminum. As the difference is not very remarkable either and all previous designs made in the VKI have used Brass, the first option is chosen.

Once the attachment and support design is fixed, it is time to resize the probe length to prevent those temperature gradients that can be seen in the second half of the probe affect the sensors (Figure 4.21). The idea is to increase the length, leaving more distance between the last sensor and the beginning of the assembly.

Parametric study for final probe length

As indicated above, the idea is to make the temperature gradient between the sensors as small as possible. For this, a parametric study will be carried out, varying the total length of the ceramic probe. As a study that only varied in length will cause different reached temperatures, the results would not be decisive. To avoid this, a final maximum temperature will be set and the heater power will be iterated until the temperature is reached. When this happens, the temperature gradient achieved will be observed. In this way, we will obtain, on the one hand, the necessary power for each of the lengths caused by a certain final maximum temperature and on the other hand, the temperature gradients produced by each study. Since the test temperatures are between 300 and 380 K, a final temperature of approximately 370 K ($\pm$1K) is established.

A COMSOL option will be used to calculate the gradient between the temperature of the hottest and least hot sensor. A type of graph is prepared, this plot shows the evolution of the temperature along the plane of symmetry of the probe for the different distances at which the sensors are located. The result is a graph with nine temperature lines. The ends of these lines to the left ($x = -3$ mm) correspond to the temperature at the stagnation point. The temperature gradient will be the subtraction between the points of the lines corresponding to the hottest and coldest sensor. An example of this graph can be found in the Figure 4.22.

Observing the Figure 4.21 it can be seen how the area where the highest temperature gradient occurs is approximately a little less than half of the probe, that is, 15 millimeters. This implies that the final length of the probe to reduce the temperature gradient reached by the sensors will be quite high, so the problem of making a hole for the heater so small and also non-concentric arises again. Therefore, it is thought to make a through-hole, so that the ceramic cylinder can be drilled from both sides, reducing the depth to be drilled in half. The parametric study will consider both cases: through-hole and non-

through hole, to see if it affects the final distribution of temperatures.

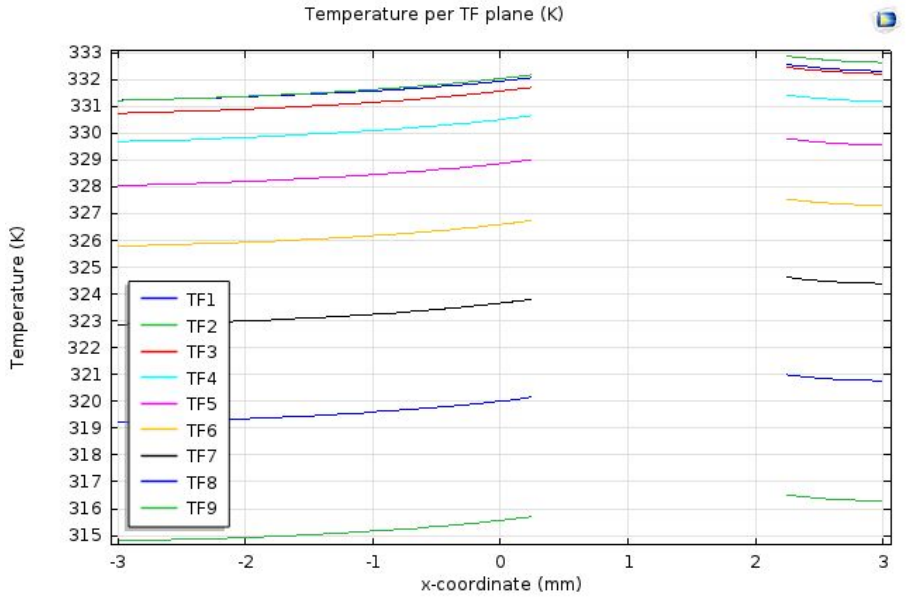

Figure 4.22: Example of plot for sensors gradient temperature calculation.

To reduce the number of images and figures in the report, the main results are summarized in Excel and plotted. The Figure 4.26 shows the different temperature gradients obtained for the different probe lengths, reaching even 70 millimeters of total length probe. The Figure 4.27 collects the different powers needed to reach maximum temperatures of 370K for the probe lengths contemplated. With these two graphs, a preliminary idea of the expected temperature gradient between the sensors for a certain length while knowing the power to be supplied by the heater can be made.

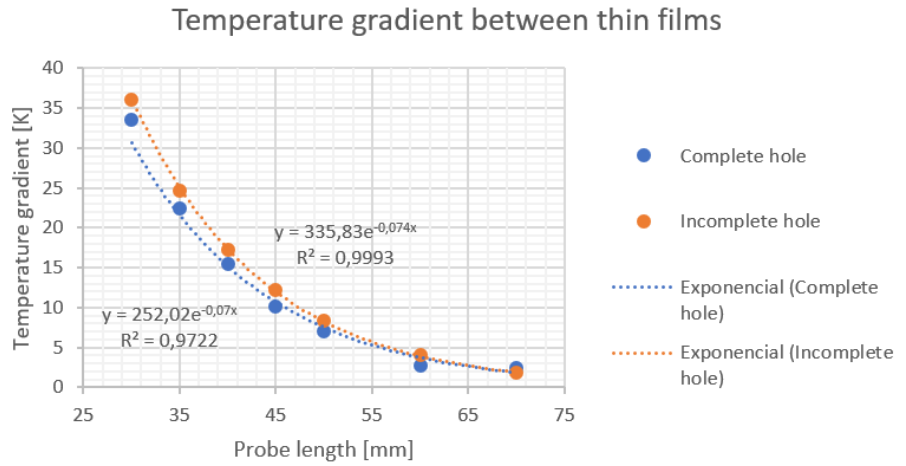

Figure 4.23: Temperature gradient between thin films vs probe length.

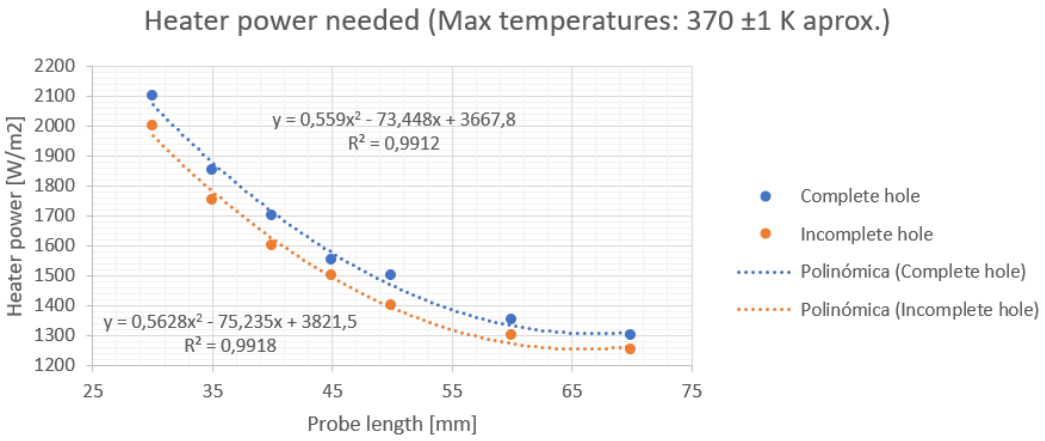

Figure 4.24: Heater power needed vs probe length.

The first conclusion that can be drawn is regarding the comparison between making a through-hole or not. The cases with through-hole provide slightly lower temperature gradients but the needed power provided by the heater is always greater, this makes sense since, being a full hole, the heater is also exposed to a part of the convection at the bottom. After seeing these results, a through-hole is chosen for the final design, since the characteristics are slightly better and the manufacturing can be greatly simplified.

The tendency of the temperature gradient with respect to the length of the probe is the expected one, decreasing. Thanks to the Figure 4.26 it can be seen the length that the probe should have for limiting the temperature gradient to a certain value. Ideally, the gradient should be reduced as much as possible, but again a balance must be found between the performance and the difficulty of making the hole in the case of a probe that is too long. The 10 millimeters corresponding to the attachment must be added to the length shown in the graphs. At the end of the project, the feasible limit length will be discussed with the technician. At the moment the design could be set at 45-50 mm. This implies a total length of the ceramic cylinder of 55-60 mm and temperature gradients of between 13 and 7 K.

As for the power supplied by the heater, it decreases as the length is increased. This makes sense since the heat flux is imposed on the entire length of the heater hole, that is, the longer, the greater the surface by which heat is supplied. For the chosen case, 45-50 mm with through-hole, the necessary power would be around 1500-1550 W/m^2.

4.8.3 Insulation

As an additional idea, the use of some material or system that allows the ceramic substrate to be isolated from the support is proposed, since as seen in the previous section, the heat losses are quite considerable.

First, the possibility of using some type of insulating material at the junction between both parties is contemplated, but at the time of carrying out the studies at COMSOL several surface overlapping problems arose. In addition, being such small elements, the available materials were limited and complicated the fabrication of the probe.

In order to quantify in some way the effects of possible thermal insulation, the following scheme is proposed in COMSOL: to leave an air chamber between the part of the attachment and the support, so that the contact surface is reduced and, with it, the heat transfer.

The same parametric study of the previous section is carried out by adding this air chamber to see if the effect is relevant or not.

In the Figure 4.25 it can be seen how the addition of the air layer affects the temperature map, delaying a little the distance at which temperature gradients take place. On the other hand, the attachment also suffers higher temperature gradients.

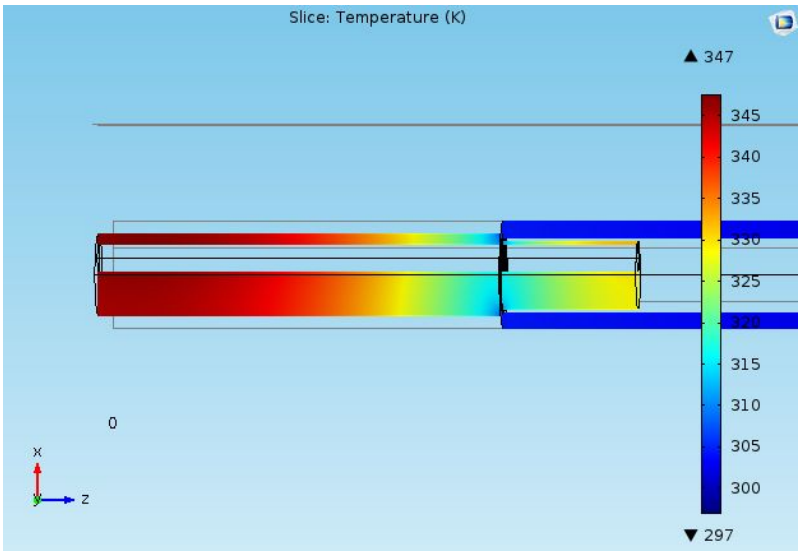

Figure 4.25: Temperature distribution for an insulated case.

Parametric study data is added to the graphs shown in the Figure 4.26 and Figure 4.27. The resulting figures are shown below:

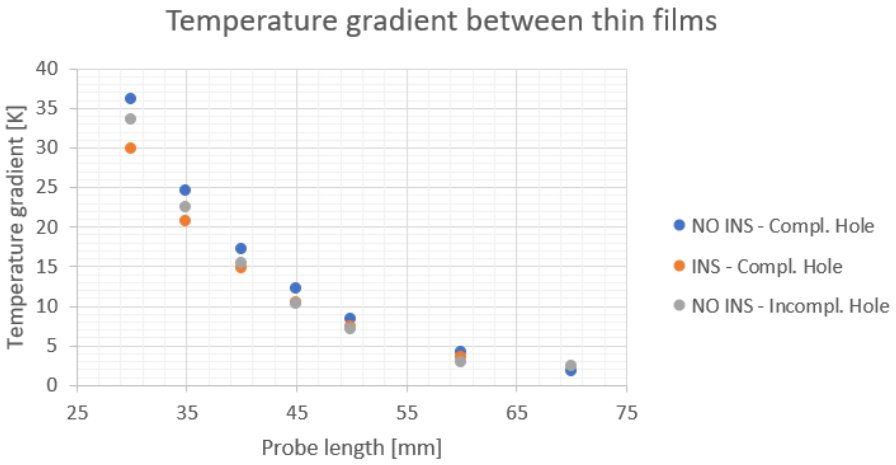

Figure 4.26: Temperature gradient between thin films vs probe length.

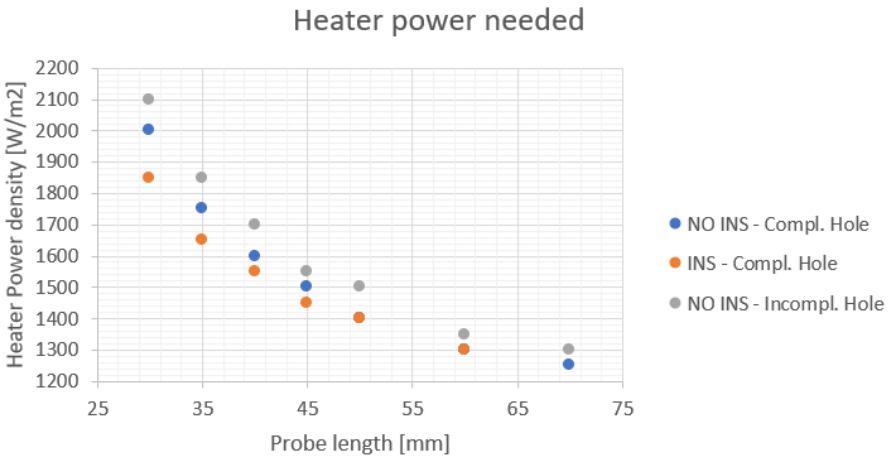

Figure 4.27: Heater power needed vs probe length.

When the length of the probe is smaller, the insulation can reduce the temperature gradient even 7K. In addition, the power required to reach a maximum temperature of 370K is also quite lower. On the other hand, as the length of the probe increases, the differences in temperature gradient are not so great, even providing practically equal results. Therefore, this section is closed proposing to eliminate the isolation between the probe and the support since it adds complexity to the design without providing a clear advantage in performance.

4.9 Final design

After compiling and considering all the sections developed so far, we proceed with the summary of the final design of the probe, which is divided into four main parts: the ceramic tip, the support, the sensors and the cabling.

The ceramic tip will be manufactured with MACOR, since it is a very machinable ceramic material and has been used in previous cases. The final dimensions are summarized in the Table 4.8. The Figure 4.28 shows the final design made with Inventor.

MACOR probe dimensions		
Length	[mm]	45-50
Diameter	[mm]	6
Heater hole (trough-out hole)		
Diameter	[mm]	2
Depth	[mm]	45-50
Distance between centers	[mm]	1.25
Cabling slot		
Depth	[mm]	0.46
Width	[mm]	3.2
Length	[mm]	45-50
Attachment		
Length	[mm]	2.5
Diameter	[mm]	10

Table 4.8: MACOR probe dimensions

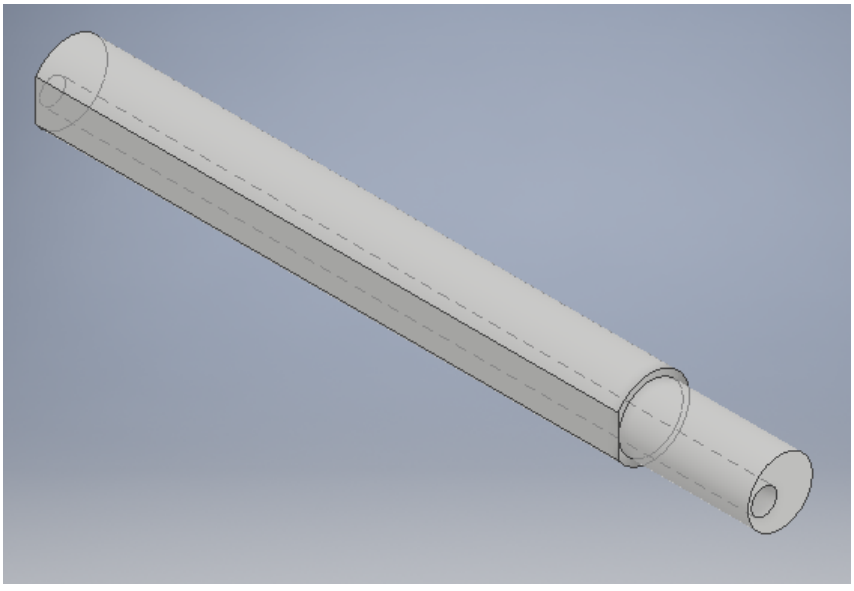

Figure 4.28: Final probe tip design.

The support will be manufactured in Brass and its dimensions are included in the Table 4.9. The Figure 4.29 shows the final design made with Inventor.

Support dimensions		
Length	[mm]	240-235
Diameter	[mm]	8
Hole (trough-out hole)		
Diameter	[mm]	2.5
Depth	[mm]	240-235
Distance between centers	[mm]	0
Cabling slot		
Depth	[mm]	0.46
Width	[mm]	3.2
Length	[mm]	12

Table 4.9: Support dimensions

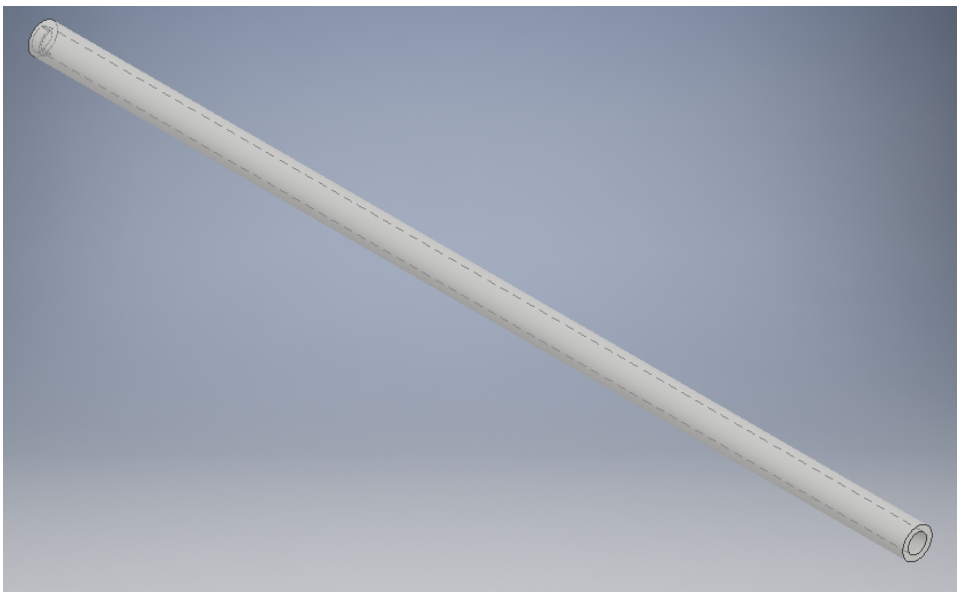

Figure 4.29: Final support design.

The sensors will be painted with platinum by the institute's technician. The characteristics of the sensors and their arrangement are shown in the Table 4.10

Thin-film sensors		
Number of sensors		9
Length	[mm]	2.1
Width	[mm]	0.9
Resistance	[Ω]	25-50
Separation	[mm]	1.9
Bottom distance	[mm]	1.6

Table 4.10: Thin-film sensors characteristics and layout

Finally, the wiring will consist of gold-painted wires from the sensor to the back of the probe. Once there, the 0.2 mm diameter cables will be welded to the golden trucks.

At the end of the project a meeting was organized with the technician in order to discuss whether the designs were feasible or not. Especially the hole for the heater. The main problem is to hold the ceramic probe to be able to make the hole correctly since the hole is not centered. At the beginning of drilling the hole, the probe starts to vibrate and those vibrations are what cause the probe to break. The hole could be made up to lengths of 50-55 millimeters. Another issue to discuss with the technician is the wiring, at first, there should be no problem with the final configuration.

To finalize the project the technical drawings of the designs can be found in tye Appendix A.

Conclusions

The designed probe will be capable of measuring temperature fluctuations up to 25kHz, or more, at the CT3 transient VKI facility. It is intended for possible use in a future experimental campaign. It is able to cover the entire span length with only 3 measurements. In each of these measurements, the probe can be reoriented thus reducing yaw angles to a minimum.

Suppose that the probe behaves as a semi-infinite solid for the calculation of heat flow is correct from probe diameters greater than 6 mm. However, it is not recommended to increase the diameter as the probe intrusiveness should be reduced. The heater must be positioned off-center to the ceramic probe in order to keep the minimum distance necessary for the semi-infinite solid hypothesis to continue to be fulfilled.

Painting sensors have clear advantages over outsourcing, including greater robustness and independence from external suppliers. The entire probe would be manufactured at the institute. The sensors are painted horizontally along the ceramic substrate.

The temperature gradient between the sensors along the probe should be reduced as much as possible. But there must be a balance between the maximum length that can be manufactured and the depth of the hole for the heater that the technician is able to make.

Finally, for the moment the idea of adding some kind of thermal insulation between the probe and the support is thrown away.

Future work

In the future, it would be necessary to carry out transitory studies in COMSOL for cases in three dimensions. In this way, the effects of the convection of the flow at the tip of the probe can be observed. At present, a distance of only 1.6 millimeters has been left between the last sensor and the end of the probe. Probably, for the transitory case, the convection in this zone will increase and affect the last sensors.

It is also proposed to redesign the transverse section of the probe. After the last meeting, it was proposed to design a non-cylindrical probe, with a rather oval cross-section. This new shape could allow more space for wiring without having to reduce both the thickness of the material in the back of the heater.

Finally, the probe will be manufactured in the laboratories of the von Karman Institute, and then calibrated in the CT3 facilities, which is where the experimental campaign will be carried out to characterize the flow of the first stages of a high-pressure turbine.

Bibliography

[1] M. C. Arenz, B. Weigel, J. Habermann, S. Staudacher, M. G. Rose, W. Berns, and E. Lutum. Development and application of a fast-response total temperature probe for turbomachinery.

[2] M. Bassignana. Design and characterization of a fast response temperature probe. Master's thesis, Politecnico di torino.

[3] T. L. Bergman, A. S. Lavine, F. P. Incropera, and D. P. Dewitt. *Fundamentals of heat and mass transfer*. John Wiley Sons, 2011.

[4] D. Buttsworth and T. Jones. A fast-response high spatial resolution total temperature probe using a pulsed heating technique.

[5] D. Buttsworth, T. Jones, and K. Chana. Unsteady total temperature measurements downstream of a high-pressure turbine.

[6] A. J. Carvalho. Development and characterization of fast-response probes for thermal measurements in high-speed turbomachinery. Master's thesis, von Karman Institute for Fluid Dynamics.

[7] COMSOL. The comsol software produc suite, August 2019.

[8] W. U. de Sevilla. Ciclo brayton, August 2019.

[9] J. Doorly and M. Oldfield. The theory of advanced multi-layer thin film heat transfer gauges.

[10] J. H. Lienhard. Sypnosis of lift, drag, and vortex frequency data for rigid circular cylinders.

[11] G. Lowery and R. Vanchon. The effect of turbulence on heat transfer from heated cylinders.

[12] M. Mansour. *A 48kHz Bandwidth, 1.8mm diameter entropy probe for aerothermal loss measurements in turbomachinery flows*. PhD thesis, Swiss Federal Institute of Technology Zurich.

[13] M. Mansour, N. Chokani, A. Kalfas, and R. Abhari. Unsteady entropy measurements in a high-speed radial compressor.

[14] M. Mansour, N. Chokani, A. I. Kalfas, and R. S. Abhari. Time-resolved entropy measurements using a fast response entropy probe.

[15] R. Merrick and G. Bitsuamlak. Control of flow around a circular cylinder by the use of surface roughness: A computation and experimental approach.

[16] A. Roshko. Experiments on the flow past a circular cylinder at very high reynolds number.

[17] E. Schmidt and K. Wenner. Wärmeabgabe über den umfang eines angeblasenen geheizten zylinders.

[18] C. Sciamanna. Calibration and data reduction of heat transfer measurements for transient turbomachinery testing. Technical report, von Karman Institute for Fluid Dynamics.

[19] Wikipedia. Ciclo brayton, August 2019.

[20] Wikipedia. Efecto termoeléctrico, August 2019.

[21] Wikipedia. Fourier number, August 2019.

[22] Wikipedia. Número de nusselt, August 2019.

[23] Wikipedia. Termopar, August 2019.

Part II

Tender dossier

Chapter 5

Occupational Health and Safety Ordinances

The general ordinance on health and safety at work is contained in BOE no. 64 of 16 March 1971. This chapter sets out the different articles of this ordinance that must be taken into account in order to preserve a suitable environment for the safe execution of work, thus avoiding risks for operators.

General rules

Article 1: Scope of application

The provisions of this Ordinance shall be adjusted to the minimum compulsory protection of persons within the scope of the Social Security System, in order to prevent accidents and occupational diseases and to achieve the best conditions of hygiene and welfare in the centers and workplaces in which such persons carry out their activities.

Article 11: Duties and rights of workers

It is the duty of the workers to cooperate in the prevention of professional risks in the Company and the maintenance of maximum hygiene in the same, to whose ends they must faithfully comply with the precepts of this Ordinance and its complementary instructions, as well as the orders and instructions that to such effects are given to them by their superiors.

Workers, expressly, are obligated to:

- To receive the teachings on Safety and Hygiene and on rescue and first

aid in the work centres provided by the Company or in the Institutions of the National Plan.

- Use personal protection equipment correctly and take care of its perfect state and conservation.
- Immediately inform their superiors of breakdowns and deficiencies that may cause hazards in any center or workplace.
- Take care of and maintain personal hygiene, avoiding contagious diseases or annoyance to co-workers.
- Submit to mandatory medical examinations and vaccinations or immunizations ordered by the competent Health Authorities or by the Company Medical Service.
- Not to introduce drinks or other substances not authorized in the workplaces, nor to appear or remain in them in a state of drunkenness or any other kind of intoxication.
- Cooperate in the extinction of claims and in the rescue of victims of occupational accidents under the conditions that, in each case, were rationally required.

Every worker, after requesting from his immediate superior the means of personal protection of a mandatory nature for the performance of his work, is empowered to delay the execution of the same, as long as such means are not provided, but must report the fact to the Health and Safety Committee or one of its components, without prejudice, in addition, to bringing it to the attention of the Provincial Labour Inspectorate.

General conditions of workplaces and protection mechanisms and measures

Article 13: Structural safety

All buildings, permanent or temporary, will be of safe and firm construction to avoid risks of collapse and those derived from atmospheric agents. To this end, the foundations, floors and other elements of the buildings shall offer sufficient resistance to support and safely suspend the loads for which they

have been calculated.

In addition, in order to preserve this security, the loads that the premises may bear or suspend shall be indicated by means of signs or inscriptions, and overloading the floors and floors of the buildings shall be prohibited.

Article 14: Surfaces and cubication

The working premises shall meet the following minimum conditions:

- Three meters high from the floor to the ceiling.
- Two square meters of surface for each worker.
- Ten cubic meters for each worker.

However, in commercial establishments, service establishments and premises for offices and offices, the height referred to in paragraph (a) of the previous number may be reduced to 2.5 m, but respecting the cubication per worker established in paragraph (c), and provided that the air is sufficiently renewed.

Space occupied by machinery, apparatus, installations and materials shall not be taken into account for the calculation of surface area and volume.

Article 15: Floors, ceilings and walls

The flooring shall constitute a homogeneous, flat and smooth whole without continuity solutions; it shall be of a consistent material, not slippery or susceptible to being slippery with use and easy to clean. In addition, it must be at the same level, and if it is not so, the differences in height will be saved by ramps with a slope of no more than 10%.

Ceilings and walls must be suitable for protecting workers from inclement weather. If they are to bear or suspend loads, they must meet the conditions laid down in Article XIII.

Article 25: Lighting. General provisions

All places of work or transit shall have natural, artificial or mixed lighting appropriate to the operations to be carried out. Use natural lighting whenever possible.

The lighting of dangerous machines, places of transit with risk of falls, stairs and emergency exits will be intensified.

Article 29: Emergency lighting

All workplaces shall be equipped with emergency lighting appropriate to the size of the premises and the number of workers occupied simultaneously, capable of maintaining, for at least one hour, an intensity of five lux by means of an energy source independent of the normal lighting system.

Article 30: Ventilation, temperature and humidity

Adequate atmospheric conditions shall be maintained in work premises and their annexes by natural or artificial means, avoiding foul air, excess heat and cold, humidity or drought and unpleasant odours.

In no case may environmental carbon dioxide exceed 50/10,000 and carbon monoxide exceed 1/10,000.

In enclosed work premises, the supply of fresh and clean air per hour and worker shall be at least 30 to 50 cubic metres unless total air renewal is carried out several times per hour, not less than six times for sedentary work and not less than ten times for work requiring more than normal physical effort.

Air circulation indoors shall be conditioned so that workers are not exposed to disturbing currents and the air speed does not exceed 15 metres per minute at normal temperature or 45 metres per minute in very hot environments.

In workplaces exposed to high and low temperatures abrupt variations will be avoided by the most effective means. When the temperature is extremely different between workplaces, there should be passageways for operators to gradually adapt to each other.

The following are set as normal limits of temperature and humidity in premises and for different jobs, provided that the manufacturing process permits:

- For sedentary jobs: From 17 to 22°C.
- For ordinary jobs: From 15 to 18°C.

- For works that require strong muscular efforts: From 12 to 15°C.

The relative humidity of the atmosphere will range from 40% to 60%, except in installations where there is danger of generating static electricity, in this case limited to 50%.

All workers shall be adequately protected against direct and excessive heat radiation. Where work is to be carried out in enclosed premises with extreme cold or heat, the permanence of operators shall be limited by establishing, where appropriate, suitable shifts.

Article 31: Noises and vibrations

Noises and vibrations shall be avoided or reduced as far as possible at their source, in an attempt to reduce their propagation in the workplace.

In this way, the anchoring of machines and devices that generate noise, vibrations and vibrations must be carried out using the most efficient techniques, in order to achieve optimum static and dynamic equilibrium, such as benches whose weight is between 1.5 and 2.5 times greater than the weight of the machine they support, due to insulation of the general structure or other technical resources.

In addition to anchoring, machines that produce annoying noises or vibrations must be properly isolated and in their enclosure, only the corresponding personnel must work for their maintenance during the indispensable time and with the equipment required to maintain the necessary safety levels.

Extreme care and maintenance must be taken of machines or equipment that produce vibrations that are annoying or dangerous to workers, especially mobile parts and devices that transmit the vibrations generated by these machines.

The control of aggressive noises in workplaces is not limited only to the isolation of the focus that produces them, but also technical precautions must be taken to prevent reflection and resonance phenomena from reaching dangerous levels for the health of workers.

Article 51: Protection against contacts in installations and in electrical equipment

In electrical installations and equipment, some of the following precautions shall be taken to protect people against contact with parts that are usually live:

- The active parts of the installation must be kept at a sufficient distance from the place where persons normally meet or travel, in order to avoid accidental contact or the handling of conductive objects, when these can be used near the installation.
- Active parts shall be coated with appropriate insulation, retaining their properties indefinitely and limiting the contact current to a harmless value.
- Obstacles shall be provided to prevent accidental contact with the active parts of the installation. Protective barriers must be securely fixed and withstand the usual mechanical stresses.

Article 57: Static Electricity

To avoid dangers from static electricity, and especially sparks in flammable environments, the following precautions should generally be taken:

- The relative humidity of the air will remain above 50%.
- The charges of static electricity that can accumulate in metal bodies will be neutralized by earth conductors.

Article 82: Fire prevention and extinction

In workplaces where there is a risk of fire, with or without an explosion, the following precautions shall be taken, combining their use with the nearest general protection provided by public fire services:

- Where there are pressurized water lines, sufficient water intakes or hydrants shall be installed at a convenient distance from each other and close to fixed work stations and personnel passage points, with appropriate hoses placed adjacent to such outlets, which shall have the appropriate cross-section and strength.

- Where pressurised water is normally lacking or insufficient, tanks should be provided with sufficient water to combat possible fires.
- In fires affecting live electrical installations, the - use of chemical foam, acid soda or water extinguishers shall be prohibited.
- Portable or mobile wheeled fire extinguishers made of physical or chemical foam, a mixture of both or dry powders, carbon dioxide or water, as appropriate to the determining cause of the fire to be extinguished, shall be provided in the vicinity of the workstations with the highest fire risk, placed in a visible and easily accessible place.
- Fire extinguishers will be periodically checked and charged according to the standards of the construction companies immediately after use.
- In order to extinguish fires that occur in magnesium and aluminium powders or chips, there should be sufficient dry fine sand, stone dust or other similar inert materials in places close to the work places. In such cases, water should never be used.
- In rooms with a high risk of fire, smoking or the introduction of matches, lighters or ignition tools is strictly forbidden. This prohibition shall be indicated by visible signs at the entrance and in the free spaces of the walls of such rooms.
- Personnel are also prohibited from introducing or using work tools, not authorised by the Company, which may cause sparks due to contact with or proximity to flammable substances.
- The use of gloves, mittens, aprons or fireproof suits, and special fire-fighting footwear that companies provide to workers for individual use is mandatory.

Part III

Costing

Chapter 1

Introducción

This budget corresponds to the project *Design of a fast-response temperature probe for turbine measurements* carried out at the von Karman Institute for Fluid Dynamics in Belgium.

The complete financing of the project, supply of computer tools, equipment, materials and human resources is carried out by the Research Institute itself, with the exception of the salary of the scholarship holder, which is the responsibility of the university of origin: Universidad Politécnica de Valencia.

This document is intended to provide an estimate of the overall amount needed to carry out the project. The budget is opened separately from the point of view of the partial cost of labour, the depreciation of the equipment necessary for its development and the fungible material used. To conclude, a compilation will be made in order to be able to provide an overall budget.

In order to be able to approach the budget it is necessary to define the duration of the project, as well as the stages and the manpower of the same one.

As for the duration of the project, the total period of the project was six months.

In terms of manpower, the project has required the direction and supervision of a contracted doctoral professor (project tutor) and the support of a doctoral student (experimental project director), in addition to the execution of the same by a scholarship holder (author of the project). All of them have a specific hourly rate.

In relation to the phases of the project, in a first stage the objectives of the project and the means to achieve them were defined. For this, the presence of the tutor and the experimental director of the project was required.

The second phase consists of the development of the project proposed in the first phase: a design of a temperature probe that meets the design requirements raised at the beginning of the project. This stage, of duration has been carried out by an aerospace engineering student. Simultaneously, frequent meetings were held in order to develop exhaustive analyses of the results obtained.

With all this you can now proceed to address an estimate of the budget that the project entails.

Chapter 2

Budget balance

The costs of the project can be divided according to the phases of the project according to the costs associated with the meetings and the costs associated with the realisation of the project itself. Following this division of costs, a balance is drawn up.

Departure from meetings

Labour, depreciation of particular equipment and some of the consumables used in the project make up the costs associated with meetings. In view of this, estimates are made.

.1 Labour costs

The labour associated with this motive mainly comprises the cost of a contracted doctoral professor, a doctoral student and a scholarship holder (author of the work), for which specific hourly rates are 50.00 €/h, 25.00 €/h and 15.00 €/h, respectively.

As mentioned above, there were meetings throughout almost the entire project period, each with different members.

The cost of the meetings relating to the establishment of the objectives, corresponding to the first phase, were carried out at the beginning of the project, with the contracted doctoral professor and the doctoral candidate acting jointly for a total time of 8 hours. This cost is shown in the Table 2.1:

Concept	Units [h]	Unit cost [€/h]	Sum [€]
Contracted professor doctor	8	50.00	400.00
Doctoral candidate	8	25	200.00
	Subtotal		**600.00**

Table 2.1: Labor cost associated with project planning meetings

The meetings corresponding to the own realisation of the project are part of the second phase. These meetings can be grouped into various types according to the people who have participated in them.

Firstly, the cost associated with the meetings between the doctoral candidate and the author of the project at a rate of 1 h/week are shown in Table 2.2.

Concept	Units [h]	Unit cost [€/h]	Sum [€]
Doctoral candidate	24	25.00	600.00
Scholarship holder	24	15.00	360.00
	Subtotal		**960.00**

Table 2.2: Labor cost associated with doctoral/grantee meetings.

Secondly, the meetings held between the contracted doctoral lecturer and the scholarship holder at a rate of 1h/month are shown in the Table. 2.3.

Concept	Units [h]	Unit cost [€/h]	Sum [€]
Contracted professor doctor	6	50.00	300.00
Scholarship holder	6	15.00	90.00
	Subtotal		**390.00**

Table 2.3: Cost of labour associated with meetings between contracted lecturer, doctor and scholarship holder.

Finally, the meetings held between contracted doctoral professor, doctoral candidate and scholarship at the rate of 1h/month are shown in the Table 2.4.

Concept	Units [h]	Unit cost [€/h]	Sum [€]
Contracted professor doctor	6	50.00	300.00
Doctoral candidate	6	25.00	150.00
Scholarship holder	6	15.00	90.00
	Subtotal		**540.00**

Table 2.4: Cost of labor associated with meetings between contracted professor, doctoral candidate and scholarship holder.

With all this, the cost associated with the labor of the item of meetings can be summarized as shown in the Table 2.5.

Concept	Units [h]	Unit cost [€/h]	Sum [€]
Contracted professor doctor	20	50.00	1000.00
Doctoral candidate	30	25.00	750.00
Scholarship holder	36	15.00	540.00
	Subtotal		**2290.00**

Table 2.5: Labour cost associated with the departure of meetings.

.2 Equipment depreciation costs

The item of meetings also involves costs due to the depreciation of the equipment used. This equipment or licences have not been acquired during and in order to obtain this work, therefore the cost of purchasing them will not be included and only the amortisation of the same during the period of the project will be recorded. In addition, the equipment used for this purpose is different from that used in other phases of the project, in particular the computer with its corresponding licences.

To simplify the balance sheet it is assumed that the equipment has a total amortization period of 5 years and that the displayed price of the licenses, purchased collectively for the entire Institute, includes 5 years of payment.

These costs are reflected in the Tables 2.6 y 2.7.

Concept	Cost [€]
Computer	700.00
Licenses	230.00

Table 2.6: Cost of equipment associated with the departure of meetings.

Cost of equipment	**930.00**	**[€]**
Amortisation period	5	[años]
Amortised period	6	[meses]
Annual amortization cost	186.00	[€]
Monthly amortization cost	15.50	[€]
Amortization cost of equipment	**93.00**	**[€]**

Table 2.7: Equipment and amortisation cost of equipment under the heading of meetings.

.3 Costs of expendable material

Finally, the item of meetings is defined taking into account the fungible material used in it, which is summarized in the Table 2.8

Concept	Units	Unit cost	Sum
	[-]	[€/ud]	[€]
Paper	100	0.01	1.00
Pen	2	0.25	0.50
	Subtotal		**1.50**

Table 2.8: Cost of consumables associated with meetings.

It is worth mentioning that these costs refer to the material that has been consumed in its entirety during the execution of the project, discarding any cost associated with material with an active useful life.

Start of validation and analysis

The concept associated with validation and analysis includes calculation and post-processing, as well as data interpretation. In addition, it requires to translate into documents the conclusions obtained from the referent analyses. Such a concept entails costs due to labour, depreciation of equipment and consumables, as well as the departure of meetings.

.1 Labour costs

Manpower corresponds to the work carried out by the author of the project during the hours estimated to have been carried out together with the doctoral student, whose hours are estimated to be 1 in 5 carried out by the scholarship holder.

Taking this into account, the cost associated with labour is shown in the Table 2.9

Concept	**Units** [h]	**Unit cost** [€/h]	**Sum** [€]
Doctoral candidate	100	25.00	2500.00
Scholarship holder	500	15.00	7500.00
	Subtotal		**10000.00**

Table 2.9: Labour cost associated with the validation and analysis item by the doctoral candidate and scholarship holder.

.2 Equipment depreciation costs

The main program used for the calculations is the COMSOL Mulitphyisics software, a private software. Therefore, the costs related to this part fall on the license and the auxiliary programs used for the post-processing of the calculations and the equipment used for it.

In view of the above, the equipment and depreciation costs thereof are summarised in the following Tables 2.10 y 2.11.

Concept	**Cost** [€]
Licencia COMOL Multiphysics	4000.00
Computer	600.00
Impresora	80.00
Microsoft Office 2018 license	230.00
Matlab 2018 license	500.00

Table 2.10: Equipment at the beginning of the validation and analysis process.

Cost of equipment	**5410**	**[€]**
Amortisation period	5	[años]
Amortized period	6	[meses]
Annual amortization cost	1082	[€]
Monthly amortization cost	90.17	[€]
Amortization cost of equipment	**541.02**	**[€]**

Table 2.11: Amortization of equipment in the computational study item.

.3 Costs of expendable material

As has been done so far, the materials consumed in this phase of the project are summarized in the following Table 2.12.

Concept	**Units**	**Unit cost**	**Sum**
	[-]	[€/ud]	[€]
Paper	150	0.01	1.50
Pen	2	0.25	0.50
Highlighter	3	0.85	2.55
	Subtotal		**4.55**

Table 2.12: Cost of consumables associated with validation and analysis.

Chapter 3

Overall budget

Finally, you can calculate the overall cost of the work on the basis of the above. This global cost has to be taken as an estimate of what it implies to fulfill the objectives of the project, and it is shown in the Table 3.1.

Concept	**Cost [€]**
Labour without VAT	12290.00
Labour incl. VAT	14870.90
Amortization of equipment	634.02
Consumable material	6.05
Total	**15510.97**

Table 3.1: Total cost of the project applied the VAT associated with the workforce.

It should be noted that labour costs do not include VAT (21.00 %), while costs associated with other items do include VAT.

Part IV

Annexes

Appendix A

Technical drawings

A (4 : 1)

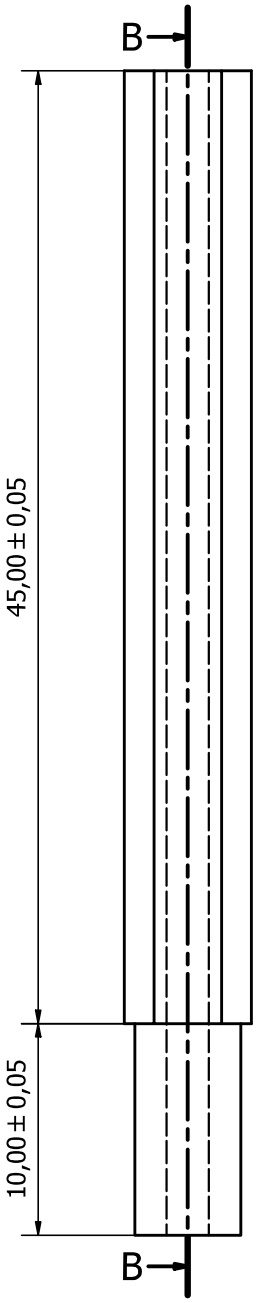

B-B (4 : 1)

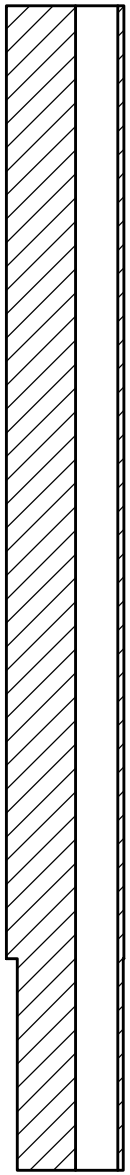

A

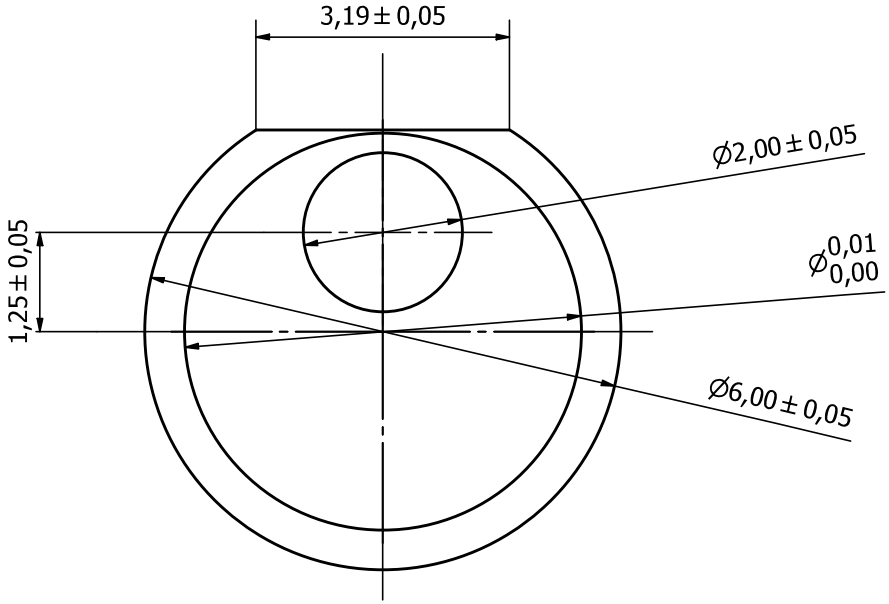

TOP (15 : 1)

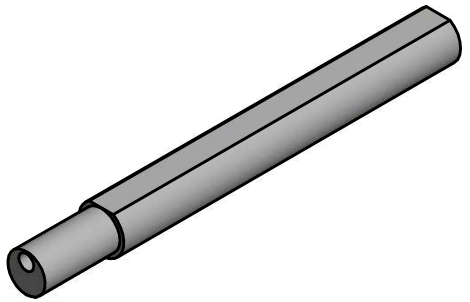

ISSOMETRIC (2 : 1)

Diseño de	Revisado por	Aprobado por	Fecha	Fecha	
NOELIA TARAZONA				05/09/2019	
von Karman Institute			MACOR Probe		
			PRONG_plano3	Edición	Hoja 1 / 1

A (1 : 1)

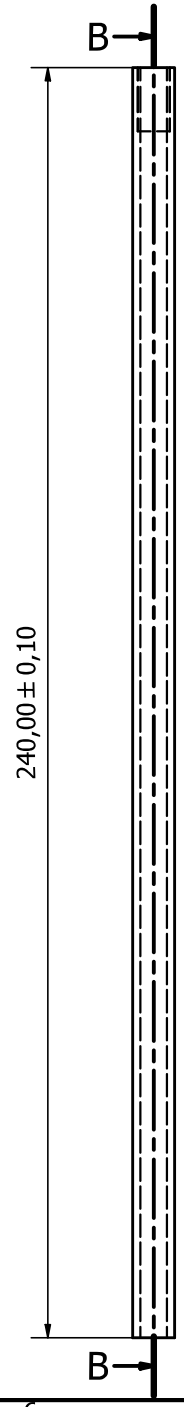

B-B (1 : 1)

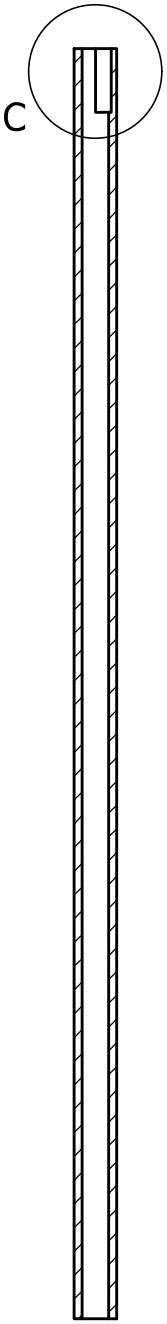

C (5 : 1)

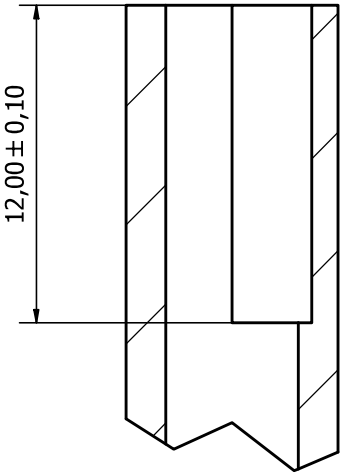

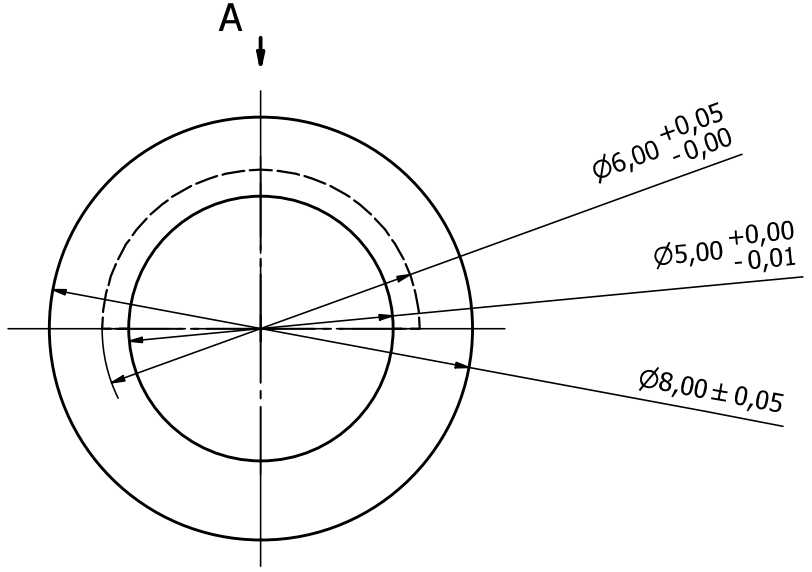

TOP (10 : 1)

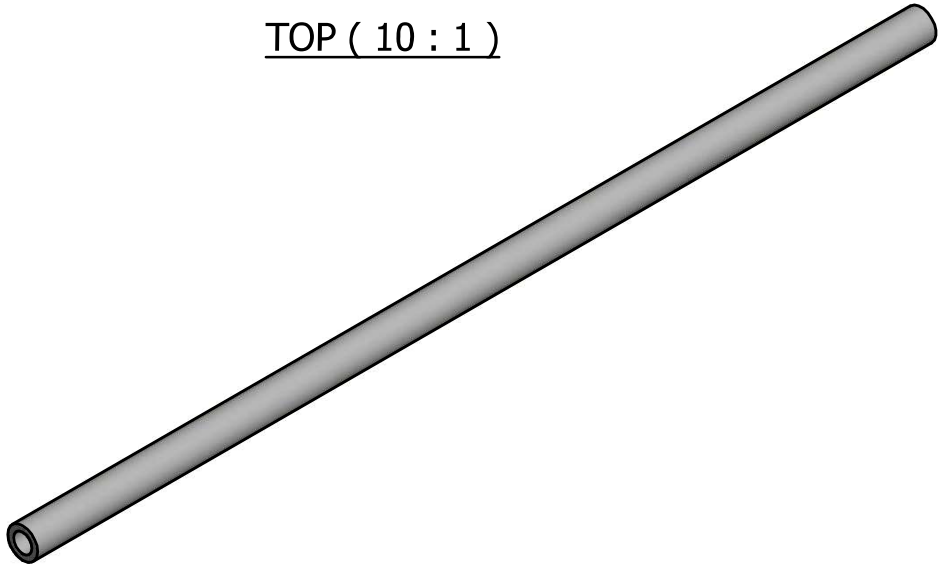

ISSOMETRIC (1 : 1)

Diseño de	Revisado por	Aprobado por	Fecha	Fecha	
NOELIA TARAZONA				05/09/2019	
von Karman Institute			Brass support		
			SUPPORT_plano	Edición	Hoja 1 / 1